Supporting Information

Molecular Dynamics Explains the Interactions Driving Sickle Cell Fibrillation

Dibyajyoti Maity[‡]*, and Debnath Pal**[‡]

[‡]Department of Computational and Data Sciences, Indian Institute of Science, Bangalore, 560012, Karnataka, INDIA

Modified CHARMM force field parameters for heme in oxyhemoglobin

The CHARMM force field parameters for heme and O_2 in oxyhemoglobin were ported to GROMACS from the AMBER parameters provided in the Supplementary information of Bringas et al.[1] These were added to the aminoacids.rtp file in the charmm27.ff force field directory in GROMACS.

```
[ HEO2 ]
 [ atoms ]
FE        FE        0.362     0
NA        NPH       -0.1      1
NB        NPH       -0.1      2
NC        NPH       -0.1      3
ND        NPH       -0.1      4
C1A       CPA       -0.04     5
C2A       CPB       0.02      6
C3A       CPB       0.02      7
C4A       CPA       -0.04     8
C1B       CPA       -0.04     9
C2B       CPB       0.02      10
C3B       CPB       0.02      11
C4B       CPA       -0.04     12
C1C       CPA       -0.04     13
C2C       CPB       0.02      14
C3C       CPB       0.02      15
C4C       CPA       -0.04     16
C1D       CPA       -0.04     17
C2D       CPB       0.02      18
C3D       CPB       0.02      19
C4D       CPA       -0.04     20
CHA       CPM       -0.12     21
HA        HA        0.16      22
CHB       CPM       -0.12     23
HB        HA        0.16      24
CHC       CPM       -0.12     25
```

```
HC        HA        0.16      26
CHD       CPM       -0.12     27
HD        HA        0.16      28
CMA       CT3       -0.227    29
HMA1      HA        0.07      30
HMA2      HA        0.07      31
HMA3      HA        0.07      32
CAA       CT2       0.05      33
HAA1      HA        0.015     34
HAA2      HA        0.015     35
CBA       CT2       -0.025    36
HBA1      HA        0.025     37
HBA2      HA        0.025     38
CGA       CC        0.635     39
O1A       OC        -0.752    40
O2A       OC        -0.752    41
CMB       CT3       -0.17     42
HMB1      HA        0.05      43
HMB2      HA        0.05      44
HMB3      HA        0.05      45
CAB       CE1       -0.08     46
HAB       HE1       0.13      47
CBB       CE2       -0.38     48
HBB1      HE2       0.15      49
HBB2      HE2       0.15      50
CMC       CT3       -0.17     51
HMC1      HA        0.05      52
HMC2      HA        0.05      53
HMC3      HA        0.05      54
CAC       CE1       -0.08     55
HAC       HE1       0.13      56
CBC       CE2       -0.38     57
HBC1      HE2       0.15      58
HBC2      HE2       0.15      59
CMD       CT3       -0.227    60
HMD1      HA        0.07      61
HMD2      HA        0.07      62
HMD3      HA        0.07      63
CAD       CT2       0.05      64
HAD1      HA        0.015     65
HAD2      HA        0.015     66
CBD       CT2       -0.025    67
HBD1      HA        0.025     68
HBD2      HA        0.025     69
CGD       CC        0.635     70
O1D       OC        -0.752    71
O2D       OC        -0.752    72
O1        OM        -0.12     73
O2        OM        -0.18     74
 [ bonds ]
FE        NA
FE        NB
```

FE	NC
FE	ND
NA	C1A
C1A	C2A
C2A	C3A
C3A	C4A
NA	C4A
C2A	CAA
CAA	CBA
CBA	CGA
CGA	O1A
CGA	O2A
C3A	CMA
CHB	C4A
CHB	C1B
NB	C1B
C1B	C2B
C2B	C3B
C3B	C4B
NB	C4B
C2B	CMB
C3B	CAB
CAB	CBB
CHC	C4B
CHC	C1C
NC	C1C
C1C	C2C
C2C	C3C
C3C	C4C
NC	C4C
C2C	CMC
C3C	CAC
CAC	CBC
CHD	C4C
CHD	C1D
ND	C1D
C1D	C2D
C2D	C3D
C3D	C4D
ND	C4D
C2D	CMD
C3D	CAD
CAD	CBD
CBD	CGD
CGD	O1D
CGD	O2D
CHA	C4D
CHA	C1A
CHA	HA
CHB	HB
CHC	HC
CHD	HD

```
CAA       HAA1
CAA       HAA2
CBA       HBA1
CBA       HBA2
CMA       HMA1
CMA       HMA2
CMA       HMA3
CMB       HMB1
CMB       HMB2
CMB       HMB3
CAB       HAB
CBB       HBB1
CBB       HBB2
CMC       HMC1
CMC       HMC2
CMC       HMC3
CAC       HAC
CBC       HBC1
CBC       HBC2
CMD       HMD1
CMD       HMD2
CMD       HMD3
CAD       HAD1
CAD       HAD2
CBD       HBD1
CBD       HBD2
O1      O2
O1      FE
 [ angles ]
;  ai    aj    ak   th0     cth     ub0    cub
   NA    FE    NC   180.0   0.0     0.0    0.0
   NB    FE    ND   180.0   0.0     0.0    0.0
   FE    O1    O2   122.0   50.00   0.0    0.0
 [ impropers ]
C2A       C1A       C3A       CAA
C3A       C2A       C4A       CMA
C2B       C1B       C3B       CMB
C3B       C2B       C4B       CAB
C2C       C1C       C3C       CMC
C3C       C2C       C4C       CAC
C2D       C1D       C3D       CMD
C3D       C2D       C4D       CAD
CGA       CBA       O2A       O1A
CGD       CBD       O2D       O1D
C4A       NA        C1A       C2A
C1A       NA        C4A       C3A
C4B       NB        C1B       C2B
C1B       NB        C4B       C3B
C4C       NC        C1C       C2C
C1C       NC        C4C       C3C
C4D       ND        C1D       C2D
C1D       ND        C4D       C3D
```

NA	C1A	C2A	C3A
NA	C4A	C3A	C2A
NB	C1B	C2B	C3B
NB	C4B	C3B	C2B
NC	C1C	C2C	C3C
NC	C4C	C3C	C2C
ND	C1D	C2D	C3D
ND	C4D	C3D	C2D
NA	C1A	CHA	C4D
NA	C4A	CHB	C1B
NB	C1B	CHB	C4A
NB	C4B	CHC	C1C
NC	C1C	CHC	C4B
NC	C4C	CHD	C1D
ND	C1D	CHD	C4C
ND	C4D	CHA	C1A
CHA	C1A	C4D	HA
CHB	C1B	C4A	HB
CHC	C1C	C4B	HC
CHD	C1D	C4C	HD
C1A	C2A	CHA	NA
C4A	C3A	CHB	NA
C1B	C2B	CHB	NB
C4B	C3B	CHC	NB
C1C	C2C	CHC	NC
C4C	C3C	CHD	NC
C1D	C2D	CHD	ND
C4D	C3D	CHA	ND
NA	C1A	C4A	FE
NB	C1B	C4B	FE
NC	C1C	C4C	FE
ND	C1D	C4D	FE

Table S1. Parameters used for MD simulation of each hemoglobin structure.

Structure	PDB ID ¶	Box length (L in Å) §	Water	Na^+	Cl^-
deoxy HbS †	2HBS	89.428	21243	49	45
deoxy HbA	2DN2	89.561	14370	38	32
deoxy HbS fibril	2HBS	266.158	402124	110	50
deoxy HbA fibril		266.390	402945	110	20
oxy HbS (T state)		89.904	14452	36	32
oxy HbA (T state)	1GZX	89.795	14449	38	32
oxy HbS (R state)		88.851	13934	35	31
oxy HbA (R state)	1HHO	88.736	13932	37	31

† The initial simulation was performed in a cubic box, which accommodated more water molecules than a rhombic dodecahedral box, leading to slower simulation. The box-type was changed to the rhombic dodecahedron for subsequent simulations to reduce the computation time.

§ The box dimensions were automatically selected by GROMACS, ensuring a minimum of 1 nm (2 nm for fibril models) distance between the protein edge and the box faces. A cube and a rhombic dodecahedron both have three equal edges so that the box dimension would be L × L × L

¶ The structures without a PDB ID were prepared in silico.

Table S2. Free energy values of the potential wells and barrier heights in the free energy landscapes of hemoglobin. The unit of energy for all columns is $kJmol^{-1}$.

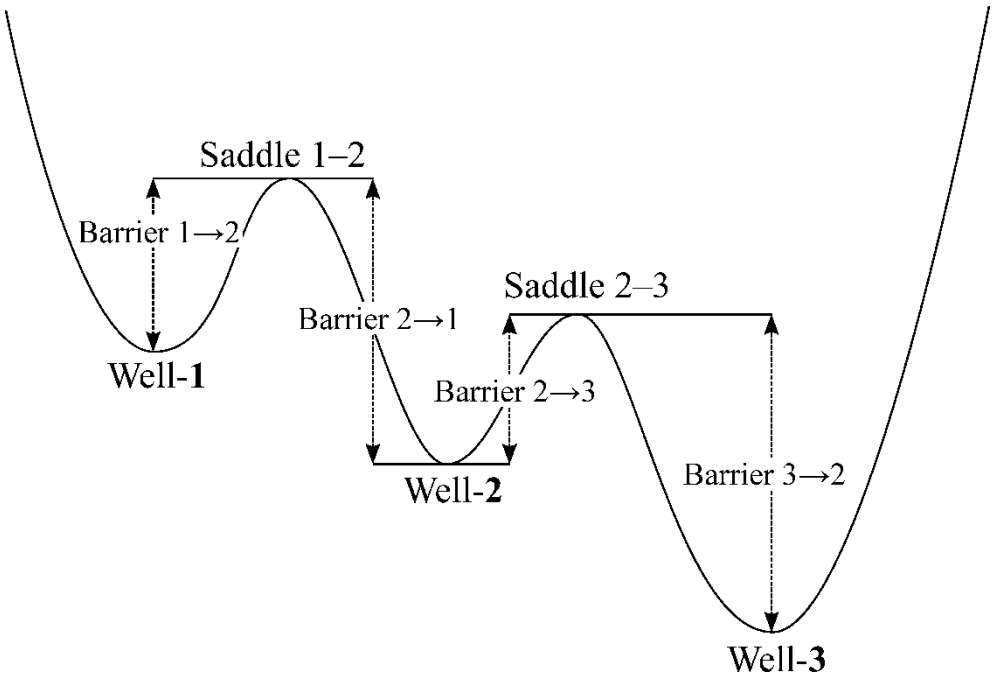

	Well-1	Barrier 1→2	Saddle 1-2	Barrier 2→1	Well-2	Barrier 2→3	Saddle 2-3	Barrier 3→2	Well-3
HbS fibril	-8.64	1.17	-7.47	5.06	-12.53				
HbA fibril	-8.03	6.30	-1.73	7.59	-9.32	2.92	-6.40	7.05	-13.45
deoxy HbS	-10.93	4.73	-6.20	7.10	-13.30	2.10	-11.20	6.01	-17.21
deoxy HbA	-9.71	3.97	-5.74	7.47	-13.21	3.71	-9.50	7.83	-17.33
oxy HbS (T)	-9.90	5.43	-4.47	4.67	-9.14	4.29	-4.85	12.88	-17.73
oxy HbA (T)	-10.08	10.08	0	5.19	-5.19	5.19	0	18.65	-18.65
oxy HbS (R)									-18.68
oxy HbA (R)									-19.86

Table S3. Outlier human hemoglobin PDB structures with dimer-dimer rotation < 70° and > 110°, which deviate from the classified T or R states.

PDB ID	Dimer-dimer rotation	Description	Comment
5HU6	48.64	Human haptoglobin-hemoglobin bound to T. Brucei haptoglobin-hemoglobin receptor	
2M6Z	113.55	Solution NMR of carboxyhemoglobin	
1CBL	113.58	Deoxy-β4 hemoglobin	β4
6FQF	114.05	Ferric-β4 hemoglobin	β4
1CBM	114.75	B4 carboxyhemoglobin	β4
1CH4	115.35	Hemoglobin with an artificial exon-shuffling, module M4-substituted	Chimera hemoglobin βα
5WOG	117.10	Hemoglobin immersed in Liquid Oxygen for 1 minute	
4WJG	129.97	Human haptoglobin-hemoglobin bound to T. Brucei haptoglobin-hemoglobin receptor	
5JDO	138.68	Human haptoglobin-hemoglobin bound to T. Congolense haptoglobin-hemoglobin receptor	
6TB2	161.75	Human haptoglobin-hemoglobin bound to S. Aureus IsdH	
4X0L	168.02	Human haptoglobin-hemoglobin bound to T. Brucei haptoglobin-hemoglobin receptor	

Table S4. The transition matrices from each hemoglobin simulation. The potential well labels are indicated on the edges of the matrices. The transition matrices were not evaluated for oxy HbS (R state) and oxy HbA (R state) because the corresponding free energy landscape has only one well.

deoxy HbS Fibril

	1	2
1	0.8434	0.1566
2	0.0262	0.9738

deoxy HbA Fibril

	1	2	3
1	0.9924	0.0076	0
2	0.0028	0.7821	0.2151
3	0	0.0386	0.9614

deoxy HbS

	1	2	3
1	0.9873	0.0127	0
2	0.0029	0.9473	0.0498
3	0	0.0079	0.9921

deoxy HbA

	1	2	3
1	0.9912	0.0088	0
2	0.0018	0.8931	0.1051
3	0	0.0166	0.9834

oxy HbS (T state)

	1	2	3
1	0.9361	0.0639	0
2	0.0229	0.9151	0.0620
3	0	0.0011	0.9989

oxy HbA (T state)

	1	2	3
1	0.9418	0.0582	0
2	0.1357	0.8369	0.0274
3	0	0.0002	0.9998

Table S5. The exact values of RMSD and R_G in Å for each potential well.

Potential Well	Well-1		Well-2		Well-3	
	RMSD (Å)	R_G (Å)	RMSD (Å)	R_G (Å)	RMSD (Å)	R_G (Å)
deoxy HbS fibril	1.81	23.81	2.54	23.97		
deoxy HbA fibril	1.76	23.55	2.59	23.56	3.36	23.62
deoxy HbS	2.02	23.51	3.26	23.69	4.04	24.06
deoxy HbA	1.50	23.76	2.79	23.72	3.21	24.17
oxy HbS (T)	1.40	23.74	2.02	23.94	3.83	24.13
oxy HbA (T)	1.86	23.90	2.90	24.20	3.93	24.22
oxy HbS (R)					2.79	24.08
oxy HbA (R)					2.22	23.71

Table S6 Comparison of contact matrix for lateral contact in which β_2-Val-6 is involved (Figure S12) with the lowest energy van der Waals interactions reported by Galamba and Pipolo[2].

1st tetramer	2nd tetramer	E_{vdW} (kJ/mol)	Observation	Comment[§]
1-β_1-Asp-73	2-β_2-Pro-5	-4.0 ± 2.6	Yes	8 in total; 1 strong
1-β_1-His-77	2-β_2-Thr-4	-4.7 ± 1.9	Yes	2 mild
1-β_1-Thr-84	2-β_2-Pro-125	-3.9 ± 1.5	Yes	3 mild
1-β_1-Leu-88	2-β_2-Val-6*	-4.4 ± 1.9	Yes	4 mild
1-β_1-Leu-88	2-β_2-Ser-9	-3.9 ± 1.9	Yes	4 in total; 1 strong
1-β_1-Heme	2-β_2-Pro-5	-4.7 ± 3.6	Yes	3 mild in HbS and 4 mild in HbA
1-β_1-Heme	2-β_2-Val-6	-5.8 ± 1.8	Yes	15 in total
1-β_2-Asn-80	2-β_2-Lys-120	-4.7 ± 2.4	No	
1-β_2-Leu-81	2-β_2-Lys-120	-5.5 ± 2.8	No	
1-β_2-Leu-81	2-β_2-Glu-121	-3.9 ± 2.1	No	

* Mutated residue in HbS

§ We have taken the liberty of associating the percentage occurrence of contacts to the strength of the contacts in the comment column. Note that the multiple points in each pair of residues in the contact matrix only mean that the atoms are positioned in a particular manner to facilitate such interactions. It is not necessarily an estimate of the contact strength between the two residues, likewise, for the contacts along a particular row or column of the contact matrix. However, residue pairs with multiple contacts with high occurrence are likely strong.

Table S7 Comparison of contact matrix for lateral contact in which β_2-Val-6 is involved (Figure S12) with the lowest energy electrostatic (attractive) interactions previously reported by Galamba and Pipolo, 2018[2] and Galamba, 2019[3].

1st tetramer	2nd tetramer	E_{pot}[2] (kJ/mol)	E_{pot}[3] (kJ/mol)	Observation	Comment[§]
1-β_1-Val-1	2-α_2-Glu-30	-127 ± 39		No	But observed in HbA
1-β_1-Lys-8	2-α_2-Glu-30	-108 ± 25		No	
1-β_1-Lys-8	2-α_2-Asp-47	-115 ± 28		No	
1-β_1-Lys-8	2-β_2-Glu-7	-110 ± 10		No	
1-β_1-Lys-65	2-β_2-Asp-79		-310 ± 86	No	But strong contacts made by 1B1-Lys66 with adjacent residue 2-B2-Leu-78
1-β_1-Asp-73	2-β_2-Lys-8	-143 ± 19		No	Asp-73 is in contact with beta-6 residue
1-β_1-Asp-73	2-β_2-Lys-132	-114 ± 30	-239 ± 37	No	
1-β_1-Asp-79	2-α_2-Lys-40		-234 ± 89	No	
1-β_1-Lys-82	2-α_2-Glu-23	-143 ± 49		No	
1-β_1-Lys-82	2-α_2-Glu-27	-172 ± 53		No	
1-β_1-Lys-82	2-α_2-Glu-30	-178 ± 61	-204 ± 110	No	
1-β_1-Lys-82	2-α_2-Asp-47		-204 ± 40	No	
1-β_1-Lys-82	2-α_2-Heme	-107 ± 8		No	
1-β_1-Lys-82	2-β_2-Glu-121	-113 ± 17		No	1-β_1-Lys-82 makes 1 mild contact with 2-β_2-Thr-123
1-β_1-Glu-90	2-β_2-Lys-17	-232 ± 91	-169 ± 51	No	But 1-β_1-Glu-90 makes 5 mild contacts with 2-β_2-Ala-13
1-β_1-Asp-94	2-β_2-Lys-17	-185 ± 55		No	
1-β_1-Lys-144	2-α_2-Glu-30		-156 ± 22	No	
1-β_1-Lys-144	2-β_2-Glu-121	-113 ± 26		**Yes**	3 mild
1-β_1-Heme	2-β_2-Val-1	-120 ± 10		No	
1-β_1-Heme	2-β_2-Lys-8	-254 ± 66	-230 ± 56	**Yes**	Observed in both HbS fibril and HbA fibril with stronger interactions in HbS fibrils.
1-β_1-Heme	2-β_2-Lys-17	-176 ± 25	-161 ± 24	No	
1-β_1-Heme	2-β_2-Lys-65	-111 ± 11		No	
1-β_1-Heme	2-β_2-Lys-132	-139 ± 15		No	
1-β_2-Val-1	2-β_2-Glu-121	-144 ± 31		No	22.7 Å Cα-Cα distance in the crystal structure
1-β_2-Asp-79	2-β_2-Lys-120	-194 ± 60		No	24.8 Å Cα-Cα distance in the crystal structure (lowest 17.8 Å terminal side-chain atoms)
1-β_2-Lys-82	2-β_2-Glu-121	-171 ± 36	-177 ± 69	No	29.9 Å Cα-Cα distance in the crystal structure
1-β_2-Asp-79	2-α_2-Arg-31	-108 ± 15		No	
1-β_2-Glu-90	2-α_2-Lys-56		-161 ± 22	No	
1-β_2-Lys-144	2-α_2-Asp-47		-313 ± 56	No	
1-β_2-Lys-144	2-α_2-Heme		-161 ± 12	No	
1-β_2-Heme	2-α_2-Lys-56	-123 ± 19	-261 ± 32	No	
1-β_2-Heme	2-α_2-Lys-60	-112 ± 18	-192 ± 29	No	

[§] We have taken the liberty of associating the percentage occurrence of contacts to the strength of the contacts in the comment column. Note that the multiple points in each pair of residues in the contact matrix only mean that the atoms are positioned in a particular manner to facilitate such interactions. Thus, it is not necessarily an estimate of the contact strength between the two residues, likewise, for the contacts along a particular row or column of the contact matrix. However, residue pairs with multiple contacts with high occurrence are likely strong.

Table S8. Correlation between interface area, interface contacts, and interface H-bonds for all simulated systems. For fibril systems, only the interfaces of the central molecule were considered.

Correlation between:	Interface area and contacts	Interface area and H-bonds	H-Bonds and contacts
deoxy HbS fibril	0.97	0.75	0.84
deoxy HbA fibril	0.99	0.59	0.62
deoxy HbS	0.99	0.46	0.52
deoxy HbA	0.99	0.91	0.89
oxy HbS (T state)	1.00	0.90	0.92
oxy HbA (T state)	0.99	0.97	0.98
oxy HbS (R state)	0.99	0.72	0.78
oxy HbA (R state)	0.99	0.73	0.78

Table S9. The hydrogen bonds in hemoglobin at various intersubunit interfaces.

	deoxy HbS Fibril			
$\alpha_1\beta_1$	α_1-Lys-99-N$^{\zeta}$—H$^{\zeta1}$	→	β_1-Tyr-35-O$^{\eta}$	36
	α_1-Lys-99-N$^{\zeta}$—H$^{\zeta1}$	→	β_1-Asn-108-O$^{\delta1}$	36
	α_1-His-103-N$^{\varepsilon2}$—H$^{\varepsilon2}$	→	β_1-Asn-108-O	39
	β_1-Arg-30-N$^{\eta2}$—H$^{\eta21}$	→	α_1-Phe-117-O	46
	β_1-Lys-120-N$^{\zeta}$—H$^{\zeta1}$	→	α_1-His-112-N$^{\delta1}$	35
	β_1-Lys-120-N$^{\zeta}$—H$^{\zeta1}$	→	α_1-His-112-O	100
	β_1-Lys-132-N$^{\zeta}$—H$^{\zeta1}$	→	α_1-Ser-35-O	93
$\alpha_2\beta_2$	α_2-Ser-35-O$^{\gamma}$—H$^{\gamma1}$	→	β_2-Gln-131-O$^{\varepsilon1}$	52
	α_2-Lys-99-N$^{\zeta}$—H$^{\zeta1}$	→	β_2-Asn-108-O$^{\delta1}$	37
	α_2-His-103-N$^{\varepsilon2}$—H$^{\varepsilon2}$	→	β_2-Asn-108-O$^{\delta1}$	54
	α_2-His-103-N$^{\varepsilon2}$—H$^{\varepsilon2}$	→	β_2-Asn-108-O	83
	α_2-His-103-N$^{\varepsilon2}$—H$^{\varepsilon2}$	→	β_2-Gln-131-N$^{\varepsilon2}$	90
	β_2-Arg-30-N$^{\varepsilon}$—H$^{\varepsilon}$	→	α_2-His-122-N$^{\delta1}$	93
	β_2-Gln-131-N$^{\varepsilon2}$—1H$^{\varepsilon2}$	→	α_2-Ser-35-O$^{\gamma}$	100
	β_2-Gln-131-N$^{\varepsilon2}$—1H$^{\varepsilon2}$	→	α_2-His-103-N$^{\delta1}$	95
$\alpha_1\beta_2$	α_1-Tyr-140-O$^{\eta}$—H$^{\eta}$	→	β_2-Trp-37-N$^{\varepsilon1}$	57
	α_1-Arg-141-N$^{\eta1}$—H$^{\eta11}$	→	β_2-Val-34-O	37
	β_2-Trp-37-N$^{\varepsilon1}$—H$^{\varepsilon1}$	→	α_1-Asp-94-O$^{\delta2}$	42
$\alpha_2\beta_1$	β_1-Trp-37-N$^{\varepsilon1}$—H$^{\varepsilon1}$	→	α_2-Asp-94-O$^{\delta2}$	45
	β_1-Arg-40-N$^{\eta1}$—H$^{\eta11}$	→	α_2-Arg-92-O	42
	β_1-Arg-40-N$^{\eta1}$—H$^{\eta11}$	→	α_2-Asp-94-O$^{\delta1}$	39
$\alpha_2\alpha_2$	α_1-Val-1-N—H^{1}	→	α_2-Arg-141-O^{T2}	86
	α_2-Val-1-N—H^{1}	→	α_1-Arg-141-O^{T2}	33
	α_2-Lys-127-N$^{\zeta}$—H$^{\zeta1}$	→	α_1-Arg-141-O^{T1}	72
	α_2-Arg-141-N$^{\eta1}$—H$^{\eta11}$	→	α_1-Asp-126-O$^{\delta2}$	55
$\beta_1\beta_2$				

	deoxy HbA Fibril			
$\alpha_1\beta_1$	α_1-Lys-99-N$^{\zeta}$—H$^{\zeta1}$	→	β_1-Glu-101-O$^{\varepsilon2}$	57
	α_1-His-103-N$^{\varepsilon2}$—H$^{\varepsilon2}$	→	β_1-Asn-108-O	44
	α_1-His-103-N$^{\varepsilon2}$—H$^{\varepsilon2}$	→	β_1-Gln-131-O$^{\varepsilon1}$	36
	α_1-His-103-N$^{\varepsilon2}$—H$^{\varepsilon2}$	→	β_1-Gln-131-N$^{\varepsilon2}$	65
	β_1-Arg-30-N$^{\eta1}$—H$^{\eta11}$	→	α_1-Phe-117-O	95
	β_1-Arg-30-N$^{\eta1}$—H$^{\eta11}$	→	α_1-His-122-N$^{\delta1}$	71
	β_1-Tyr-35-O$^{\eta}$—H$^{\eta}$	→	α_1-Asp-126-O$^{\delta1}$	31
	β_1-Gln-131-N$^{\varepsilon2}$—1H$^{\varepsilon2}$	→	α_1-Ser-35-O$^{\gamma}$	100
	β_1-Lys-132-N$^{\zeta}$—H$^{\zeta1}$	→	α_1-Leu-34-O	94
$\alpha_2\beta_2$	α_2-Lys-99-N$^{\zeta}$—H$^{\zeta1}$	→	β_2-Glu-101-O$^{\varepsilon2}$	54
	α_2-His-103-N$^{\varepsilon2}$—H$^{\varepsilon2}$	→	β_2-Asn-108-O	33
	α_2-His-103-N$^{\varepsilon2}$—H$^{\varepsilon2}$	→	β_2-Gln-131-N$^{\varepsilon2}$	70
	β_2-Arg-30-N$^{\eta1}$—H$^{\eta11}$	→	α_2-Phe-117-O	67
	β_2-Arg-30-N$^{\eta2}$—H$^{\eta21}$	→	α_2-Thr-118-O	54
	β_2-Arg-30-N$^{\eta2}$—H$^{\eta21}$	→	α_2-His-122-N$^{\delta1}$	43
	β_2-Gln-131-N$^{\varepsilon2}$—1H$^{\varepsilon2}$	→	α_2-Ser-35-O$^{\gamma}$	100
	β_2-Lys-132-N$^{\zeta}$—H$^{\zeta1}$	→	α_2-Leu-34-O	95
$\alpha_1\beta_2$	α_1-Arg-92-N$^{\eta1}$—H$^{\eta11}$	→	β_2-Glu-43-O$^{\varepsilon2}$	97
	α_1-Arg-92-N$^{\eta2}$—H$^{\eta21}$	→	β_2-Glu-43-O$^{\varepsilon2}$	50
	α_1-Asn-97-N$^{\delta2}$—1H$^{\delta2}$	→	β_2-Asp-99-O$^{\delta1}$	46
	α_1-Arg-141-N$^{\eta1}$—H$^{\eta11}$	→	β_2-Val-34-O	35
	α_1-Arg-141-N$^{\eta2}$—H$^{\eta21}$	→	β_2-Tyr-35-O$^{\eta}$	32
	β_2-Asn-102-N$^{\delta2}$—1H$^{\delta2}$	→	α_1-Asp-94-O$^{\delta1}$	42
	β_2-Asn-102-N$^{\delta2}$—1H$^{\delta2}$	→	α_1-Asp-94-O$^{\delta2}$	41
$\alpha_2\beta_1$	β_1-Trp-37-N$^{\varepsilon1}$—H$^{\varepsilon1}$	→	α_2-Asp-94-O$^{\delta1}$	74
	β_1-Arg-40-N$^{\eta1}$—H$^{\eta11}$	→	α_2-Thr-41-O	38
	β_1-Arg-40-N$^{\eta1}$—H$^{\eta11}$	→	α_2-Asp-94-O$^{\delta2}$	36
	β_1-Arg-40-N$^{\eta2}$—H$^{\eta21}$	→	α_2-Thr-41-O$^{\gamma1}$	43
	α_2-Arg-92-N$^{\eta2}$—H$^{\eta21}$	→	β_1-Pro-36-O	66
	α_2-Arg-92-N$^{\eta2}$—H$^{\eta21}$	→	β_1-Gln-39-O$^{\varepsilon1}$	47
$\alpha_2\alpha_2$	α_1-Val-1-N—H^{1}	→	α_2-Ser-138-O	40
	α_1-Val-1-N—H^{1}	→	α_2-Arg-141-O^{T2}	61
	α_1-Lys-127-N$^{\zeta}$—H$^{\zeta1}$	→	α_2-Arg-141-O^{T1}	38
	α_1-Arg-141-N$^{\eta1}$—H$^{\eta11}$	→	α_2-Asp-126-O$^{\delta1}$	62
	α_1-Arg-141-N$^{\eta1}$—H$^{\eta11}$	→	α_2-Asp-126-O$^{\delta2}$	40
	α_1-Arg-141-N$^{\eta2}$—H$^{\eta21}$	→	α_2-Asp-126-O$^{\delta1}$	34
	α_2-Val-1-N—H1	→	α_1-Ser-138-O	76
	α_2-Lys-127-N$^{\zeta}$—H$^{\zeta1}$	→	α_1-Arg-141-O^{T2}	95
	α_2-Arg-141-N$^{\eta1}$—H$^{\eta11}$	→	α_1-Asp-126-O$^{\delta1}$	49
	α_2-Arg-141-N$^{\eta1}$—H$^{\eta11}$	→	α_1-Asp-126-O$^{\delta2}$	51
	α_2-Arg-141-N$^{\eta2}$—H$^{\eta21}$	→	α_1-Asp-126-O$^{\delta1}$	37
	α_2-Arg-141-N$^{\eta2}$—H$^{\eta21}$	→	α_1-Asp-126-O$^{\delta2}$	60
$\beta_1\beta_2$	β_1-Arg-104-N$^{\eta1}$—H$^{\eta11}$	→	β_2-Glu-101-O$^{\varepsilon2}$	48
	β_1-Arg-104-N$^{\eta2}$—H$^{\eta21}$	→	β_2-Glu-101-O$^{\varepsilon1}$	50
	β_2-His-146-N$^{\varepsilon2}$—H$^{\varepsilon2}$	→	β_1-His-2-N$^{\varepsilon2}$	49
	β_2-His-146-N$^{\varepsilon2}$—H$^{\varepsilon2}$	→	β_1-Ala-135-O	45

	deoxy HbS			
$\alpha_1\beta_1$	β_1-Gln-131-N$^{\varepsilon2}$—H$^{\varepsilon12}$	→	α_1-His-103-N$^{\delta1}$	100
	β_1-Lys-132-N$^{\zeta}$—H$^{\zeta1}$	→	α_1-Ser-35-O	95
$\alpha_2\beta_2$	α_2-His-103-N$^{\varepsilon2}$—H$^{\varepsilon2}$	→	β_2-Gln-131-O$^{\varepsilon1}$	49
	β_2-Arg-30-N$^{\varepsilon}$—H$^{\varepsilon}$	→	α_2-His-122-N$^{\delta1}$	37
	β_2-Arg-30-N$^{\varepsilon}$—H$^{\varepsilon}$	→	α_2-His-122-N$^{\varepsilon2}$	50
	β_2-Arg-30-N$^{\eta2}$—H$^{\eta21}$	→	α_2-Phe-117-O	80
	β_2-Arg-30-N$^{\eta2}$—H$^{\eta21}$	→	α_2-His-122-N$^{\delta1}$	76
	β_2-Tyr-35-O$^{\eta}$—H$^{\eta}$	→	α_2-Asp-126-O$^{\delta2}$	93
	β_2-Gln-131-N$^{\varepsilon2}$—H$^{\varepsilon12}$	→	α_2-His-103-N$^{\delta1}$	100
	β_2-Lys-132-N$^{\zeta}$—H$^{\zeta1}$	→	α_2-Ser-35-O	94
$\alpha_1\beta_2$	α_1-Arg-92-N$^{\varepsilon}$—H$^{\varepsilon}$	→	β_2-Pro-36-O	34
	α_1-Tyr-140-O$^{\eta}$—H$^{\eta}$	→	β_2-Trp-37-N$^{\varepsilon1}$	38
	β_2-Arg-40-N$^{\eta1}$—H$^{\eta11}$	→	α_1-Thr-41-O	46
	β_2-Arg-40-N$^{\eta2}$—H$^{\eta21}$	→	α_1-Thr-41-O	50
	β_2-Arg-40-N$^{\eta2}$—H$^{\eta21}$	→	α_1-Tyr-42-O$^{\eta}$	46
	β_2-Arg-40-N$^{\eta2}$—H$^{\eta21}$	→	α_1-His-89-N$^{\delta1}$	48
	β_2-Arg-40-N$^{\eta2}$—H$^{\eta21}$	→	α_1-His-89-O	50
$\alpha_2\beta_1$	α_2-Arg-92-N$^{\varepsilon}$—H$^{\varepsilon}$	→	β_1-Gln-39-O$^{\varepsilon1}$	54
	α_2-Arg-92-N$^{\eta2}$—H$^{\eta21}$	→	β_1-Pro-36-O	57
	α_2-Arg-92-N$^{\eta2}$—H$^{\eta21}$	→	β_1-Gln-39-O$^{\varepsilon1}$	33
	α_2-Arg-92-N$^{\eta2}$—H$^{\eta21}$	→	β_1-Gln-39-O	42
$\alpha_2\alpha_2$	α_1-Val-1-N—H^{1}	→	α_2-Arg-141-O^{T2}	34
	α_1-Ser-3-O$^{\gamma}$—H$^{\eta21}$	→	α_2-Arg-141-O^{T2}	40
	α_1-Thr-134-O$^{\gamma1}$—H$^{\gamma1}$	→	α_2-Arg-141-N$^{\eta1}$	34
	α_1-Arg-141-N$^{\eta2}$—H$^{\eta21}$	→	α_2-Ala-123-O	46
	α_1-Arg-141-N$^{\eta2}$—H$^{\eta21}$	→	α_2-Asp-126-O$^{\delta1}$	52
	α_2-Val-1-N—H^{1}	→	α_1-Ser-138-O$^{\gamma}$	67
	α_2-Val-1-N—H^{1}	→	α_1-Lys-139-O	35
	α_2-Val-1-N—H^{1}	→	α_1-Arg-141-O^{T1}	62
	α_2-Ser-131-O$^{\gamma}$—H$^{\gamma1}$	→	α_1-Arg-141-O^{T1}	38
$\beta_1\beta_2$	β_1-His-146-N$^{\varepsilon2}$—H$^{\varepsilon2}$	→	β_2-Asn-139-O$^{\delta1}$	37
	β_1-His-146-N$^{\varepsilon2}$—H$^{\varepsilon2}$	→	β_2-Asn-139-N$^{\delta2}$	36
	β_2-His-146-N$^{\varepsilon2}$—H$^{\varepsilon2}$	→	β_1-Gly-136-N	39
	β_2-His-146-N$^{\varepsilon2}$—H$^{\varepsilon2}$	→	β_1-Asn-139-O$^{\delta1}$	41

	deoxy HbA			
$\alpha_1\beta_1$	α_1-His-103-N$^{\varepsilon2}$—H$^{\varepsilon2}$	→	β_1-Gln-131-O$^{\varepsilon1}$	47
	β_1-Arg-30-N$^{\eta1}$—H$^{\eta11}$	→	α_1-His-122-N$^{\delta1}$	68
	β_1-Arg-30-N$^{\eta2}$—H$^{\eta21}$	→	α_1-Phe-117-O	69
	β_1-Tyr-35-O$^{\eta}$—H$^{\eta}$	→	α_1-Asp-126-O$^{\delta1}$	95
	β_1-Asn-108-N$^{\delta2}$—H$^{\delta21}$	→	α_1-His-103-N$^{\delta1}$	70
	β_1-Gln-131-N$^{\varepsilon2}$—H$^{\varepsilon12}$	→	α_1-Ser-35-O$^{\gamma}$	31
	β_1-Gln-131-N$^{\varepsilon2}$—H$^{\varepsilon12}$	→	α_1-His-103-N$^{\delta1}$	100
	β_1-Lys-132-N$^{\zeta}$—H$^{\zeta1}$	→	α_1-Ser-35-O	93
$\alpha_2\beta_2$	α_2-His-103-N$^{\varepsilon2}$—H$^{\varepsilon2}$	→	β_2-Gln-131-O$^{\varepsilon1}$	56
	β_2-Arg-30-N$^{\eta2}$—H$^{\eta21}$	→	α_2-Phe-117-O	52
	β_2-Arg-30-N$^{\eta2}$—H$^{\eta21}$	→	α_2-Thr-118-O	44
	β_2-Arg-30-N$^{\eta2}$—H$^{\eta21}$	→	α_2-Pro-119-N	98
	β_2-Tyr-35-O$^{\eta}$—H$^{\eta}$	→	α_2-Asp-126-O$^{\delta2}$	73
	β_2-Asn-108-N$^{\delta2}$—H$^{\delta21}$	→	α_2-His-103-N$^{\delta1}$	67
	β_2-Gln-131-N$^{\varepsilon2}$—H$^{\varepsilon12}$	→	α_2-His-103-N$^{\delta1}$	100
	β_2-Lys-132-N$^{\zeta}$—H$^{\zeta1}$	→	α_2-Ser-35-O	95
$\alpha_1\beta_2$	α_1-Thr-41-O$^{\gamma1}$—H$^{\gamma1}$	→	β_2-His-97-N$^{\delta1}$	43
	α_1-Thr-41-O$^{\gamma1}$—H$^{\gamma1}$	→	β_2-His-97-N$^{\varepsilon2}$	52
	α_1-Tyr-42-O$^{\eta}$—H$^{\eta}$	→	β_2-His-97-N$^{\delta1}$	38
	α_1-Arg-92-N$^{\eta2}$—H$^{\eta21}$	→	β_2-Gln-39-O$^{\varepsilon1}$	75
	α_1-Asn-97-N$^{\delta2}$—H$^{\delta1}$2	→	β_2-Asp-99-O$^{\delta1}$	34
	α_1-Asn-97-N$^{\delta2}$—H$^{\delta1}$2	→	β_2-Asp-99-O$^{\delta2}$	37
	β_2-Trp-37-N—H	→	α_1-Tyr-140-O	34
$\alpha_2\beta_1$	β_1-Trp-37-N$^{\varepsilon1}$—H$^{\varepsilon1}$	→	α_2-Asp-94-O$^{\delta2}$	68
	β_1-Arg-40-N$^{\eta1}$—H$^{\eta11}$	→	α_2-Ala-88-O	39
	β_1-Arg-40-N$^{\eta1}$—H$^{\eta11}$	→	α_2-His-89-N$^{\delta1}$	37
	β_1-Arg-40-N$^{\eta1}$—H$^{\eta11}$	→	α_2-Asp-94-O$^{\delta2}$	39
	β_1-Arg-40-N$^{\eta1}$—H$^{\eta11}$	→	α_2-Tyr-140-O$^{\eta}$	41
	α_2-Thr-41-O$^{\gamma1}$—H$^{\gamma1}$	→	β_1-His-97-N$^{\delta1}$	79
	α_2-Arg-92-N$^{\eta2}$—H$^{\eta21}$	→	β_1-Pro-36-O	78
$\alpha_2\alpha_2$	α_1-Val-1-N—H^{1}	→	α_2-Ser-138-O	84
	α_2-Lys-127-N$^{\zeta}$—H$^{\zeta1}$	→	α_1-Arg-141-O^{T2}	56
	α_2-Arg-141-N$^{\varepsilon}$—H$^{\varepsilon}$	→	α_1-Asp-126-O$^{\delta2}$	43
$\beta_1\beta_2$				

	oxy HbS (T state)			
$\alpha_1\beta_1$	α_1-His-103-N$^{\varepsilon2}$—H$^{\varepsilon2}$	→	β_1-Tyr-35-O$^{\eta}$	58
	α_1-His-103-N$^{\varepsilon2}$—H$^{\varepsilon2}$	→	β_1-Asn-108-O	41
	α_1-His-103-N$^{\varepsilon2}$—H$^{\varepsilon2}$	→	β_1-Gln-127-N$^{\varepsilon2}$	46
	α_1-His-103-N$^{\varepsilon2}$—H$^{\varepsilon2}$	→	β_1-Gln-131-O$^{\varepsilon1}$	98
	β_1-Arg-30-N$^{\eta2}$—H$^{\eta21}$	→	α_1-Phe-117-O	69
	β_1-Arg-30-N$^{\eta2}$—H$^{\eta21}$	→	α_1-Thr-118-O	74
	β_1-Lys-120-N$^{\zeta}$—H$^{\zeta1}$	→	α_1-His-112-O	38
	β_1-Gln-127-N$^{\varepsilon2}$—1H$^{\varepsilon2}$	→	α_1-Cys-104-O	100
	β_1-Lys-132-N$^{\zeta}$—H$^{\zeta1}$	→	α_1-Ser-35-O	92
$\alpha_2\beta_2$	α_2-Lys-99-N$^{\zeta}$—H$^{\zeta1}$	→	β_2-Asn-108-N$^{\delta2}$	50
	α_2-His-103-N$^{\varepsilon2}$—H$^{\varepsilon2}$	→	β_2-Cys-112-N	35
	α_2-His-103-N$^{\varepsilon2}$—H$^{\varepsilon2}$	→	β_2-Gln-127-N$^{\varepsilon2}$	46
	α_2-His-103-N$^{\varepsilon2}$—H$^{\varepsilon2}$	→	β_2-Gln-131-N$^{\varepsilon2}$	93
	β_2-Arg-30-N$^{\eta1}$—H$^{\eta11}$	→	α_2-Phe-117-O	65
	β_2-Arg-30-N$^{\eta2}$—H$^{\eta21}$	→	α_2-Phe-117-O	67
	β_2-Lys-120-N$^{\zeta}$—H$^{\zeta1}$	→	α_2-His-112-O	37
	β_2-Gln-131-N$^{\varepsilon2}$—1H$^{\varepsilon2}$	→	α_2-Ser-35-O	100
	β_2-Lys-132-N$^{\zeta}$—H$^{\zeta1}$	→	α_2-Ser-35-O	92
$\alpha_1\beta_2$	α_1-Lys-40-N$^{\zeta}$—H$^{\zeta1}$	→	β_2-His-146-O^{T2}	53
	α_1-Tyr-42-O$^{\eta}$—H$^{\eta}$	→	β_2-Arg-40-N$^{\eta1}$	32
	α_1-Tyr-42-O$^{\eta}$—H$^{\eta}$	→	β_2-Arg-40-N$^{\eta2}$	65
	α_1-Arg-92-N$^{\eta2}$—H$^{\eta21}$	→	β_2-Gln-39-O$^{\varepsilon1}$	64
$\alpha_2\beta_1$	β_1-Trp-37-N$^{\varepsilon1}$—H$^{\varepsilon1}$	→	α_2-Asp-94-O$^{\delta2}$	69
	β_1-Arg-40-N$^{\eta1}$—H$^{\eta11}$	→	α_2-Thr-41-O	38
	β_1-Arg-40-N$^{\eta1}$—H$^{\eta11}$	→	α_2-Tyr-42-O$^{\eta}$	39
	β_1-Arg-40-N$^{\eta1}$—H$^{\eta11}$	→	α_2-Arg-92-O	39
	β_1-Arg-40-N$^{\eta1}$—H$^{\eta11}$	→	α_2-Asp-94-N	37
	α_2-Thr-41-O$^{\gamma1}$—H$^{\gamma1}$	→	β_1-Tyr-145-O$^{\eta}$	48
	α_2-Tyr-42-O$^{\eta}$—H$^{\eta}$	→	β_1-Arg-40-N$^{\varepsilon}$	53
	α_2-Arg-92-N$^{\eta1}$—H$^{\eta11}$	→	β_1-Arg-40-N$^{\eta2}$	46
	α_2-Arg-92-N$^{\eta1}$—H$^{\eta11}$	→	β_1-Arg-40-O	51
$\alpha_2\alpha_2$	α_1-Val-1-N—H^{1}	→	α_2-Ser-138-O	46
	α_1-Lys-127-N$^{\zeta}$—H$^{\zeta1}$	→	α_2-Arg-141-O^{T1}	59
	α_1-Lys-127-N$^{\zeta}$—H$^{\zeta1}$	→	α_2-Arg-141-O^{T2}	38
	α_2-Ser-3-O$^{\gamma}$—H$^{\gamma1}$	→	α_1-Arg-141-O^{T1}	46
	α_2-Lys-127-N$^{\zeta}$—H$^{\zeta1}$	→	α_1-Arg-141-O^{T2}	74
$\beta_1\beta_2$	β_1-Arg-104-N$^{\varepsilon}$—H$^{\varepsilon}$	→	β_2-His-146-O^{T1}	44
	β_1-Arg-104-N$^{\varepsilon}$—H$^{\varepsilon}$	→	β_2-His-146-O^{T2}	43
	β_1-Arg-104-N$^{\eta1}$—H$^{\eta11}$	→	β_2-His-146-N$^{\varepsilon2}$	44
	β_1-Arg-104-N$^{\eta1}$—H$^{\eta11}$	→	β_2-His-146-O^{T1}	45
	β_2-Asn-139-N$^{\delta2}$—1H$^{\delta2}$	→	β_1-His-143-O	36
	β_2-Asn-139-N$^{\delta2}$—1H$^{\delta2}$	→	β_1-Tyr-145-O	34

	oxy HbA (T state)			
$\alpha_1\beta_1$	α_1-Ser-35-O$^{\gamma}$—H$^{\gamma1}$	→	β_1-Gln-131-O$^{\varepsilon1}$	55
	α_1-Lys-99-N$^{\zeta}$—H$^{\zeta1}$	→	β_1-Arg-104-N$^{\eta2}$	39
	α_1-Lys-99-N$^{\zeta}$—H$^{\zeta1}$	→	β_1-Asn-108-O$^{\delta1}$	52
	α_1-Lys-99-N$^{\zeta}$—H$^{\zeta1}$	→	β_1-Asn-108-N$^{\delta2}$	92
	α_1-His-103-N$^{\varepsilon2}$—H$^{\varepsilon2}$	→	β_1-Asn-108-O	66
	α_1-His-103-N$^{\varepsilon2}$—H$^{\varepsilon2}$	→	β_1-Gln-127-N$^{\varepsilon2}$	67
	β_1-Lys-120-N$^{\zeta}$—H$^{\zeta1}$	→	α_1-His-112-N$^{\delta1}$	36
	β_1-Gln-127-N$^{\varepsilon2}$—1H$^{\varepsilon2}$	→	α_1-Arg-31-O	100
	β_1-Gln-131-N$^{\varepsilon2}$—1H$^{\varepsilon2}$	→	α_1-His-103-N$^{\delta1}$	93
$\alpha_2\beta_2$	α_2-Lys-99-N$^{\zeta}$—H$^{\zeta1}$	→	β_2-Glu-101-O$^{\varepsilon2}$	57
	α_2-His-103-N$^{\varepsilon2}$—H$^{\varepsilon2}$	→	β_2-Gln-131-O$^{\varepsilon1}$	46
	α_2-His-103-N$^{\varepsilon2}$—H$^{\varepsilon2}$	→	β_2-Gln-131-N$^{\varepsilon2}$	38
	α_2-Phe-117-N—H	→	β_2-His-116-N$^{\varepsilon2}$	96
	β_2-Arg-30-N$^{\eta2}$—H$^{\eta21}$	→	α_2-Phe-117-O	71
	β_2-Arg-30-N$^{\eta2}$—H$^{\eta21}$	→	α_2-Thr-118-O	70
	β_2-Gln-127-N$^{\varepsilon2}$—1H$^{\varepsilon2}$	→	α_2-Arg-31-O	33
	β_2-Gln-131-N$^{\varepsilon2}$—1H$^{\varepsilon2}$	→	α_2-His-103-N$^{\delta1}$	100
	β_2-Lys-132-N$^{\zeta}$—H$^{\zeta1}$	→	α_2-Ser-35-O	92
$\alpha_1\beta_2$	α_1-Tyr-42-O$^{\eta}$—H$^{\eta}$	→	β_2-Arg-40-N$^{\varepsilon}$	43
	α_1-Tyr-42-O$^{\eta}$—H$^{\eta}$	→	β_2-Asp-99-O$^{\delta2}$	44
	α_1-Arg-141-N$^{\eta2}$—H$^{\eta21}$	→	β_2-Tyr-35-O$^{\eta}$	64
	β_2-Arg-40-N$^{\varepsilon}$—H$^{\varepsilon}$	→	α_1-Arg-92-N$^{\eta2}$	38
	β_2-Arg-40-N$^{\varepsilon}$—H$^{\varepsilon}$	→	α_1-Tyr-140-O$^{\eta}$	36
	β_2-Arg-40-N$^{\eta1}$—H$^{\eta11}$	→	α_1-Lys-90-O	34
	β_2-Arg-40-N$^{\eta1}$—H$^{\eta11}$	→	α_1-Leu-91-O	37
$\alpha_2\beta_1$	β_1-Gln-39-N$^{\varepsilon2}$—1H$^{\varepsilon2}$	→	α_2-Arg-92-N$^{\eta1}$	69
	β_1-Arg-40-N$^{\varepsilon}$—H$^{\varepsilon}$	→	α_2-Asp-94-O$^{\delta2}$	44
	β_1-Arg-40-N$^{\eta1}$—H$^{\eta11}$	→	α_2-Thr-41-O	33
	β_1-Arg-40-N$^{\eta1}$—H$^{\eta11}$	→	α_2-Val-93-O	33
	β_1-Arg-40-N$^{\eta1}$—H$^{\eta11}$	→	α_2-Asp-94-O$^{\delta1}$	44
	α_2-Thr-41-O$^{\gamma1}$—H$^{\gamma1}$	→	β_1-His-97-N$^{\delta1}$	42
	α_2-Thr-41-O$^{\gamma1}$—H$^{\gamma1}$	→	β_1-Val-98-O	59
	α_2-Arg-92-N$^{\eta1}$—H$^{\eta11}$	→	β_1-Arg-40-O	54
	α_2-Arg-92-N$^{\eta1}$—H$^{\eta11}$	→	β_1-Glu-43-O$^{\varepsilon1}$	34
$\alpha_2\alpha_2$	α_1-Val-1-N—H^{1}	→	α_2-Ser-138-O	46
	α_1-Val-1-N—H^{1}	→	α_2-Arg-141-O^{T1}	65
	α_1-Val-1-N—H^{1}	→	α_2-Arg-141-O^{T2}	32
	α_2-Val-1-N—H^{1}	→	α_1-Ser-138-O	46
	α_2-Val-1-N—H^{1}	→	α_1-Arg-141-O^{T1}	72
$\beta_1\beta_2$	β_1-Val-1-N—H^{1}	→	β_2-His-146-O^{T2}	51
	β_1-His-146-N$^{\varepsilon2}$—H$^{\varepsilon2}$	→	β_2-Asn-139-O$^{\delta1}$	56
	β_1-His-146-N$^{\varepsilon2}$—H$^{\varepsilon2}$	→	β_2-Asn-139-O	57
	β_2-Val-1-N—H^{1}	→	β_1-His-146-O^{T2}	56
	β_2-His-143-N$^{\varepsilon2}$—H$^{\varepsilon2}$	→	β_1-His-146-O^{T2}	51
	β_2-His-146-N$^{\varepsilon2}$—H$^{\varepsilon2}$	→	β_1-Asn-139-O$^{\delta1}$	54

	oxy HbS (R state)			
$\alpha_1\beta_1$	α_1-His-103-N$^{\varepsilon2}$—H$^{\varepsilon2}$	→	β_1-Gln-131-O$^{\varepsilon1}$	41
	α_1-Lys-127-N$^{\zeta}$—H$^{\zeta1}$	→	β_1-Val-34-O	41
	β_1-Arg-30-N$^{\eta1}$—H$^{\eta11}$	→	α_1-Phe-117-O	51
	β_1-Arg-30-N$^{\eta1}$—H$^{\eta11}$	→	α_1-Thr-118-O	81
	β_1-Arg-30-N$^{\eta1}$—H$^{\eta11}$	→	α_1-Pro-119-N	98
	β_1-Tyr-35-O$^{\eta}$—H$^{\eta}$	→	α_1-Asp-126-O$^{\delta1}$	65
	β_1-His-116-N$^{\varepsilon2}$—H$^{\varepsilon2}$	→	α_1-Ala-115-O	31
	β_1-Gln-131-N$^{\varepsilon2}$—1H$^{\varepsilon2}$	→	α_1-Ser-35-O$^{\gamma}$	39
	β_1-Gln-131-N$^{\varepsilon2}$—1H$^{\varepsilon2}$	→	α_1-His-103-N$^{\delta1}$	100
	β_1-Lys-132-N$^{\zeta}$—H$^{\zeta1}$	→	α_1-Ser-35-O	93
$\alpha_2\beta_2$	α_2-His-103-N$^{\varepsilon2}$—H$^{\varepsilon2}$	→	β_2-Asn-108-O	46
	α_2-Lys-127-N$^{\zeta}$—H$^{\zeta1}$	→	β_2-Val-33-O	62
	β_2-Gln-127-N$^{\varepsilon2}$—1H$^{\varepsilon2}$	→	α_2-Thr-108-O$^{\gamma1}$	34
	β_2-Gln-131-N$^{\varepsilon2}$—1H$^{\varepsilon2}$	→	α_2-His-103-N$^{\delta1}$	100
	β_2-Lys-132-N$^{\zeta}$—H$^{\zeta1}$	→	α_2-Ser-35-O	92
$\alpha_1\beta_2$	α_1-Thr-38-O$^{\gamma1}$—H$^{\gamma1}$	→	β_2-Asp-99-O$^{\delta1}$	49
	α_1-Thr-38-O$^{\gamma1}$—H$^{\gamma1}$	→	β_2-Asp-99-O$^{\delta2}$	48
	α_1-Thr-41-O$^{\gamma1}$—H$^{\gamma1}$	→	β_2-His-97-N$^{\delta1}$	35
	α_1-Thr-41-O$^{\gamma1}$—H$^{\gamma1}$	→	β_2-His-97-N$^{\varepsilon2}$	64
	α_1-Tyr-42-O$^{\eta}$—H$^{\eta}$	→	β_2-Arg-40-N$^{\varepsilon}$	88
	α_1-Arg-92-N$^{\eta2}$—H$^{\eta21}$	→	β_2-Gly-46-O	34
	α_1-Arg-92-N$^{\eta2}$—H$^{\eta21}$	→	β_2-Asp-47-O$^{\delta1}$	33
$\alpha_2\beta_1$	β_1-Tyr-35-O$^{\eta}$—H$^{\eta}$	→	α_2-Arg-141-N$^{\eta2}$	55
	α_2-Lys-40-N$^{\zeta}$—H$^{\zeta1}$	→	β_1-His-97-N$^{\delta1}$	69
	α_2-Arg-92-N$^{\eta1}$—H$^{\eta11}$	→	β_1-Arg-40-N$^{\eta1}$	66
$\alpha_2\alpha_2$	α_1-Val-1-N—H^{1}	→	α_2-Ser-138-O	40
	α_1-Val-1-N—H^{1}	→	α_2-Lys-139-O	60
	α_2-Val-1-N—H^{1}	→	α_1-Ser-138-O$^{\gamma}$	35
	α_2-Val-1-N—H^{1}	→	α_1-Ser-138-O	36
$\beta_1\beta_2$	β_1-Arg-104-N$^{\eta2}$—H$^{\eta21}$	→	β_2-Glu-101-O$^{\varepsilon1}$	31
	β_1-Asn-139-N$^{\delta2}$—1H$^{\delta2}$	→	β_2-Tyr-145-O$^{\eta}$	41
	β_1-Asn-139-N$^{\delta2}$—1H$^{\delta2}$	→	β_2-Tyr-145-O	42
	β_1-His-143-N$^{\varepsilon2}$—H$^{\varepsilon2}$	→	β_2-Lys-82-N$^{\zeta}$	39
	β_1-His-143-N$^{\varepsilon2}$—H$^{\varepsilon2}$	→	β_2-His-143-N$^{\delta1}$	38
	β_2-Lys-144-N$^{\zeta}$—H$^{\zeta1}$	→	β_1-His-2-N$^{\delta1}$	39
	β_2-Tyr-145-O$^{\eta}$—H$^{\eta}$	→	β_1-Asn-139-O$^{\delta1}$	39

	oxy HbA (R state)			
$\alpha_1\beta_1$	β_1-Arg-30-N$^{\eta1}$—H$^{\eta11}$	→	α_1-Thr-118-O	33
	β_1-Arg-30-N$^{\eta1}$—H$^{\eta11}$	→	α_1-Pro-119-N	37
	β_1-Arg-30-N$^{\eta1}$—H$^{\eta11}$	→	α_1-His-122-N$^{\delta1}$	82
	β_1-Arg-30-N$^{\eta2}$—H$^{\eta21}$	→	α_1-Phe-117-O	99
	β_1-Asn-108-N$^{\delta2}$—1H$^{\delta2}$	→	α_1-His-103-N$^{\delta1}$	58
	β_1-His-116-N$^{\varepsilon2}$—H$^{\varepsilon2}$	→	α_1-Ala-115-O	46
	β_1-Gln-131-N$^{\varepsilon2}$—1H$^{\varepsilon2}$	→	α_1-His-103-N$^{\delta1}$	100
	β_1-Lys-132-N$^{\zeta}$—H$^{\zeta1}$	→	α_1-Ser-35-O	96
$\alpha_2\beta_2$	α_2-His-103-N$^{\varepsilon2}$—H$^{\varepsilon2}$	→	β_2-Asn-108-O$^{\delta1}$	35
	α_2-His-103-N$^{\varepsilon2}$—H$^{\varepsilon2}$	→	β_2-Gln-127-N$^{\varepsilon2}$	47
	α_2-His-103-N$^{\varepsilon2}$—H$^{\varepsilon2}$	→	β_2-Gln-131-O$^{\varepsilon1}$	60
	α_2-His-103-N$^{\varepsilon2}$—H$^{\varepsilon2}$	→	β_2-Gln-131-N$^{\varepsilon2}$	49
	α_2-Phe-117-N—H	→	β_2-His-116-N$^{\varepsilon2}$	85
	α_2-Lys-127-N$^{\zeta}$—H$^{\zeta1}$	→	β_2-Val-34-O	69
	β_2-Gln-127-N$^{\varepsilon2}$—1H$^{\varepsilon2}$	→	α_2-His-103-O	34
	β_2-Gln-131-N$^{\varepsilon2}$—1H$^{\varepsilon2}$	→	α_2-Ser-35-O	100
	β_2-Lys-132-N$^{\zeta}$—H$^{\zeta1}$	→	α_2-Leu-34-O	94
$\alpha_1\beta_2$	α_1-Thr-41-O$^{\gamma1}$—H$^{\gamma1}$	→	β_2-His-97-N$^{\varepsilon2}$	39
	α_1-Tyr-42-O$^{\eta}$—H$^{\eta}$	→	β_2-Arg-40-N$^{\varepsilon}$	37
	α_1-Tyr-42-O$^{\eta}$—H$^{\eta}$	→	β_2-Asp-99-O$^{\delta2}$	33
	α_1-Arg-92-N$^{\varepsilon}$—H$^{\varepsilon}$	→	β_2-Arg-40-N$^{\eta1}$	32
	α_1-Arg-141-N$^{\varepsilon}$—H$^{\varepsilon}$	→	β_2-Val-34-O	45
$\alpha_2\beta_1$	β_1-Arg-40-N$^{\varepsilon}$—H$^{\varepsilon}$	→	α_2-Leu-91-O	49
	β_1-Arg-40-N$^{\eta1}$—H$^{\eta11}$	→	α_2-Thr-41-O$^{\gamma1}$	48
	β_1-Arg-40-N$^{\eta1}$—H$^{\eta11}$	→	α_2-Asp-94-N	35
	β_1-Arg-40-N$^{\eta1}$—H$^{\eta11}$	→	α_2-Asp-94-O$^{\delta1}$	38
	α_2-Thr-38-O$^{\gamma1}$—H$^{\gamma1}$	→	β_1-Asp-99-O$^{\delta2}$	37
	α_2-Arg-92-N$^{\varepsilon}$—H$^{\varepsilon}$	→	β_1-Gln-39-O	58
	α_2-Arg-92-N$^{\varepsilon}$—H$^{\varepsilon}$	→	β_1-Glu-43-O$^{\varepsilon1}$	46
	α_2-Arg-92-N$^{\eta1}$—H$^{\eta11}$	→	β_1-Gln-39-O	46
	α_2-Arg-92-N$^{\eta1}$—H$^{\eta11}$	→	β_1-Glu-43-O$^{\varepsilon1}$	58
	α_2-Arg-92-N$^{\eta2}$—H$^{\eta21}$	→	β_1-Gln-39-O$^{\varepsilon1}$	78
$\alpha_2\alpha_2$	α_1-Arg-141-N$^{\varepsilon}$—H$^{\varepsilon}$	→	α_2-Asp-126-O$^{\delta2}$	36
	α_1-Arg-141-N$^{\varepsilon}$—H$^{\varepsilon}$	→	α_2-Lys-127-O	36
	α_1-Arg-141-N$^{\eta1}$—H$^{\eta11}$	→	α_2-Asp-126-O$^{\delta2}$	50
	α_1-Arg-141-N$^{\eta1}$—H$^{\eta11}$	→	α_2-Thr-134-O$^{\gamma1}$	58
	α_2-Arg-141-N$^{\eta1}$—H$^{\eta11}$	→	α_1-Ala-130-O	52
	α_2-Arg-141-N$^{\eta1}$—H$^{\eta11}$	→	α_1-Ser-131-O$^{\gamma}$	48
	α_2-Arg-141-N$^{\eta2}$—H$^{\eta21}$	→	α_1-Asp-126-O$^{\delta1}$	52
	α_2-Arg-141-N$^{\eta2}$—H$^{\eta21}$	→	α_1-Asp-126-O$^{\delta2}$	47
	α_2-Arg-141-N$^{\eta2}$—H$^{\eta21}$	→	α_1-Thr-134-O$^{\gamma1}$	45
$\beta_1\beta_2$	β_1-Asn-139-N$^{\delta2}$—1H$^{\delta2}$	→	β_2-His-146-N$^{\delta1}$	56
	β_1-Asn-139-N$^{\delta2}$—1H$^{\delta2}$	→	β_2-His-146-N$^{\varepsilon2}$	55
	β_2-Val-1-N—H^{1}	→	β_1-Asp-94-O$^{\delta1}$	38

Table S10. The Average backbone RMSF over all residues in a chain and the complete tetramer for various hemoglobin simulations. RMSF is greater in β chains than the α chains for deoxyhemoglobin, but it is similar for oxyhemoglobins. The 'All residues' column contains the mean of RSMF for all residues in each molecule. The column 'Whole' lists the backbone RMSF of the complete tetramer. Moreover, these values are higher because they include the contribution from inter-subunit motions.

	α_1 chain	β_1 chain	α_2 chain	β_2 chain	All residues	Whole
HbS Fibril	0.59 ± 0.24	0.66 ± 0.38	0.55 ± 0.20	0.77 ± 0.34	0.65 ± 0.31	0.96 ± 0.39
HbA Fibril	0.55 ± 0.18	0.61 ± 0.20	0.57 ± 0.18	0.63 ± 0.22	0.59 ± 0.20	0.93 ± 0.31
deoxy HbS	0.60 ± 0.24	0.76 ± 0.31	0.59 ± 0.22	0.70 ± 0.27	0.66 ± 0.27	1.12 ± 0.32
deoxy HbA	0.58 ± 0.24	0.83 ± 0.49	0.56 ± 0.21	0.71 ± 0.36	0.67 ± 0.36	1.05 ± 0.41
oxy HbS (T)	0.62 ± 0.32	0.64 ± 0.23	0.62 ± 0.28	0.73 ± 0.31	0.65 ± 0.29	1.07 ± 0.35
oxy HbA (T)	0.64 ± 0.35	0.68 ± 0.32	0.61 ± 0.30	0.64 ± 0.24	0.64 ± 0.30	1.06 ± 0.37
oxy HbS (R)	0.60 ± 0.33	0.82 ± 0.37	0.70 ± 0.37	0.91 ± 0.45	0.76 ± 0.40	1.08 ± 0.43
oxy HbA (R)	0.66 ± 0.32	0.68 ± 0.27	0.58 ± 0.21	0.63 ± 0.20	0.64 ± 0.26	0.89 ± 0.31

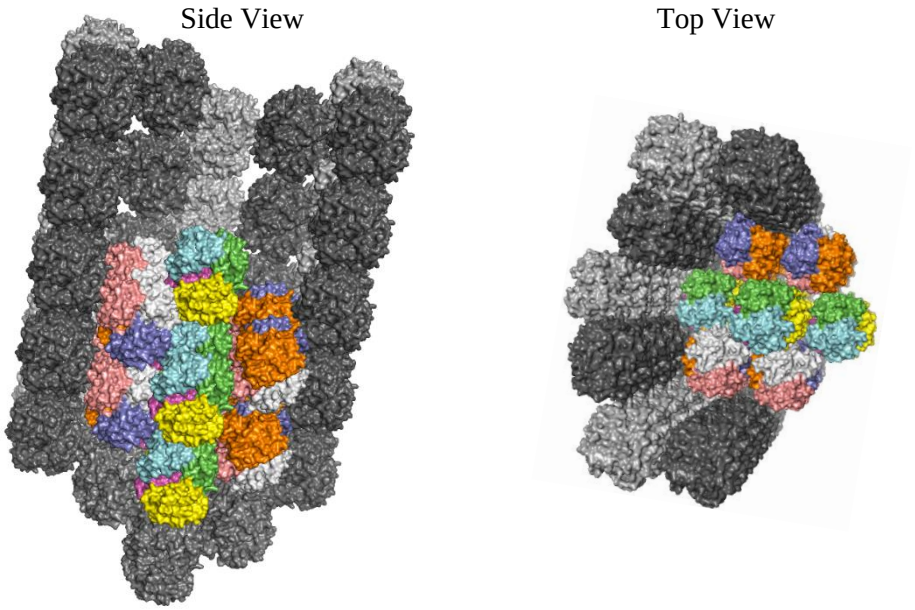

Figure S1 A schematic showing the substructure of the putative HbS fibril model (a 14-stranded model obtained from computer reconstruction of electron micrographs[4-9]) for which the MD simulation was performed (HbS Fibril). Barring a slight helical twist, the structure of the 14-stranded model closely resembles the packing in the HbS crystal. The 15 colored HbS tetramer arrangement was the structure used

in the MD simulation of the HbS Fibril in this study. For clarity, some of the tetramers towards the top of the schematic have not been displayed, and the strands have been colored in alternate shades of gray. The chains of the first tetramer in the unit cell are colored: α_1=green, β_1=cyan, α_2=magenta, and β_2=yellow. The chains of the second tetramer in the unit cell are colored: α_1=pink, β_1=white, α_2=purple, and β_2=orange.

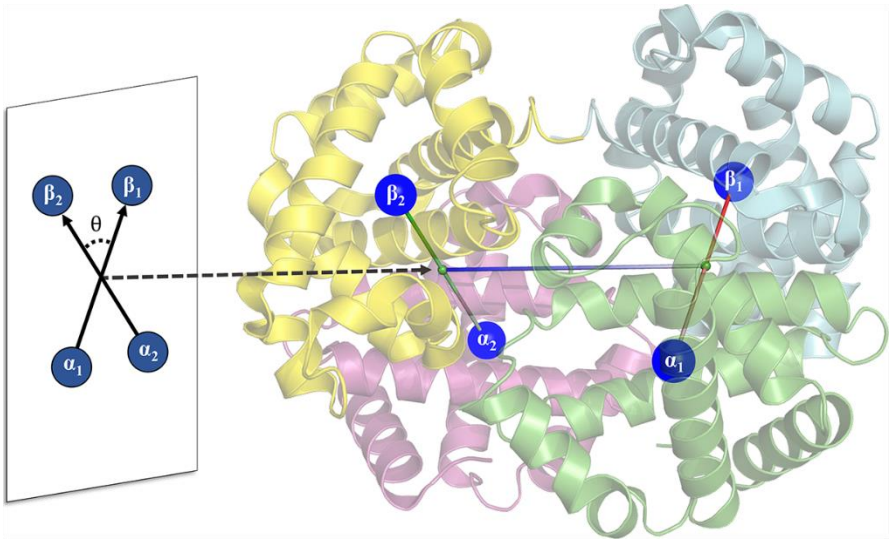

Figure S2. Hemoglobin dimer-dimer rotation and separation. The center of mass of each chain in the hemoglobin, the $\alpha_1\beta_1$ dimer, and the $\alpha_2\beta_2$ dimer was evaluated. The vector from the center of mass of α_1 to the center of mass of β_1 was calculated. Likewise, for the vector from α_2 to β_2. The projections of these vectors were taken on the plane normal to the vector from the center of mass of $\alpha_1\beta_1$ dimer to the center of mass of $\alpha_2\beta_2$ dimer. The angle between these two projections is the dimer rotation (θ). The distance between the center of masses $\alpha_1\beta_1$ and $\alpha_2\beta_2$ dimers is the dimer separation.

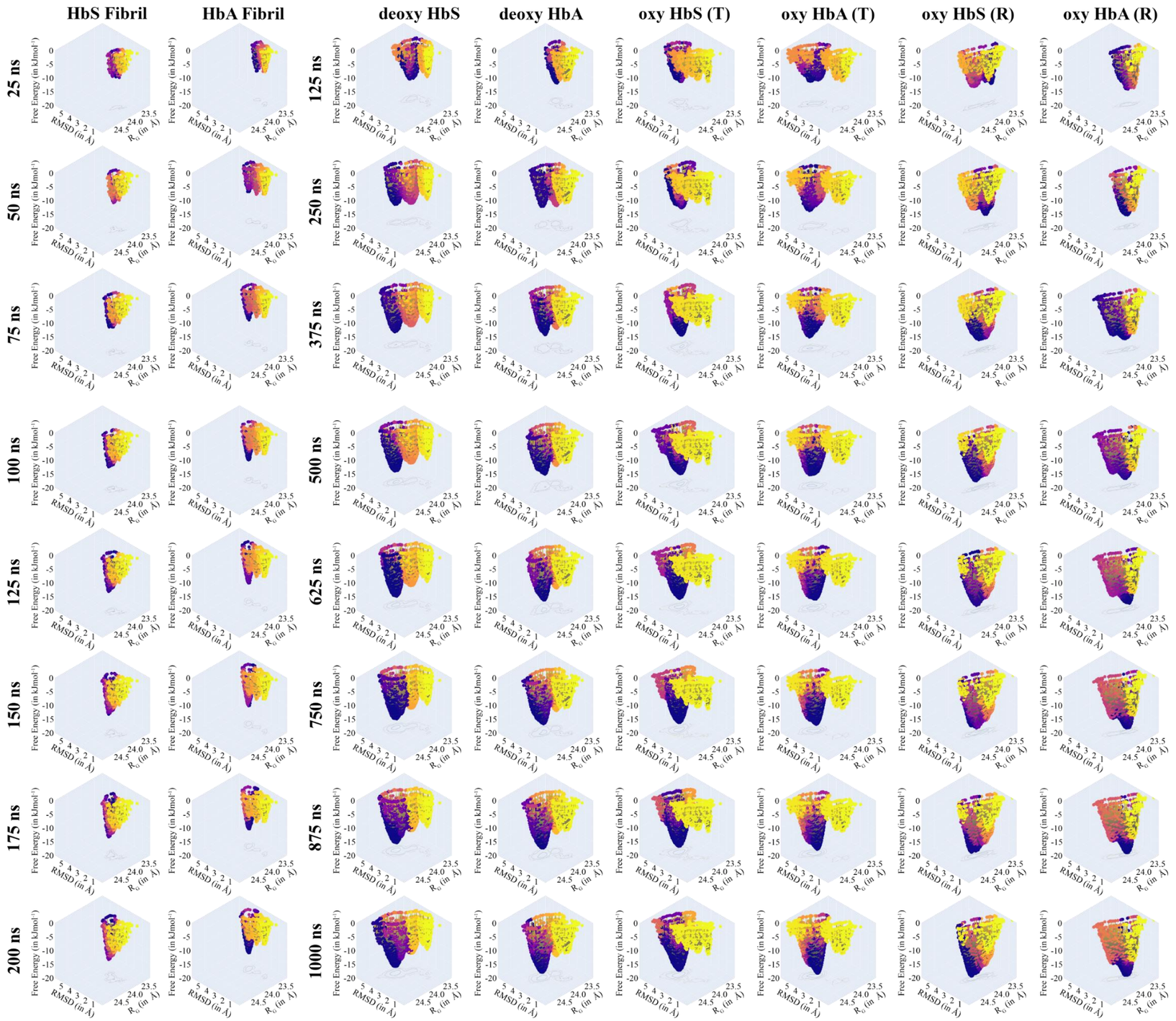

Figure S3 Evolution of free energy landscapes from the hemoglobin MD simulations. For each hemoglobin fibril simulation, free energy landscapes were created using the trajectories till 25 ns, 50 ns, …, 200 ns. Moreover, free energy landscapes for each hemoglobin tetramer simulation were created using the trajectories till 125 ns, 250 ns, …, 1000 ns. The landscapes are on the same ranges and energy scale for each case, with 100 bins in each dimension. Beyond 625 ns for single tetramer simulation and beyond 125 ns for fibril simulations, there is very little change in the features of the free energy landscapes, demonstrating that the entire trajectory had been adequately sampled.

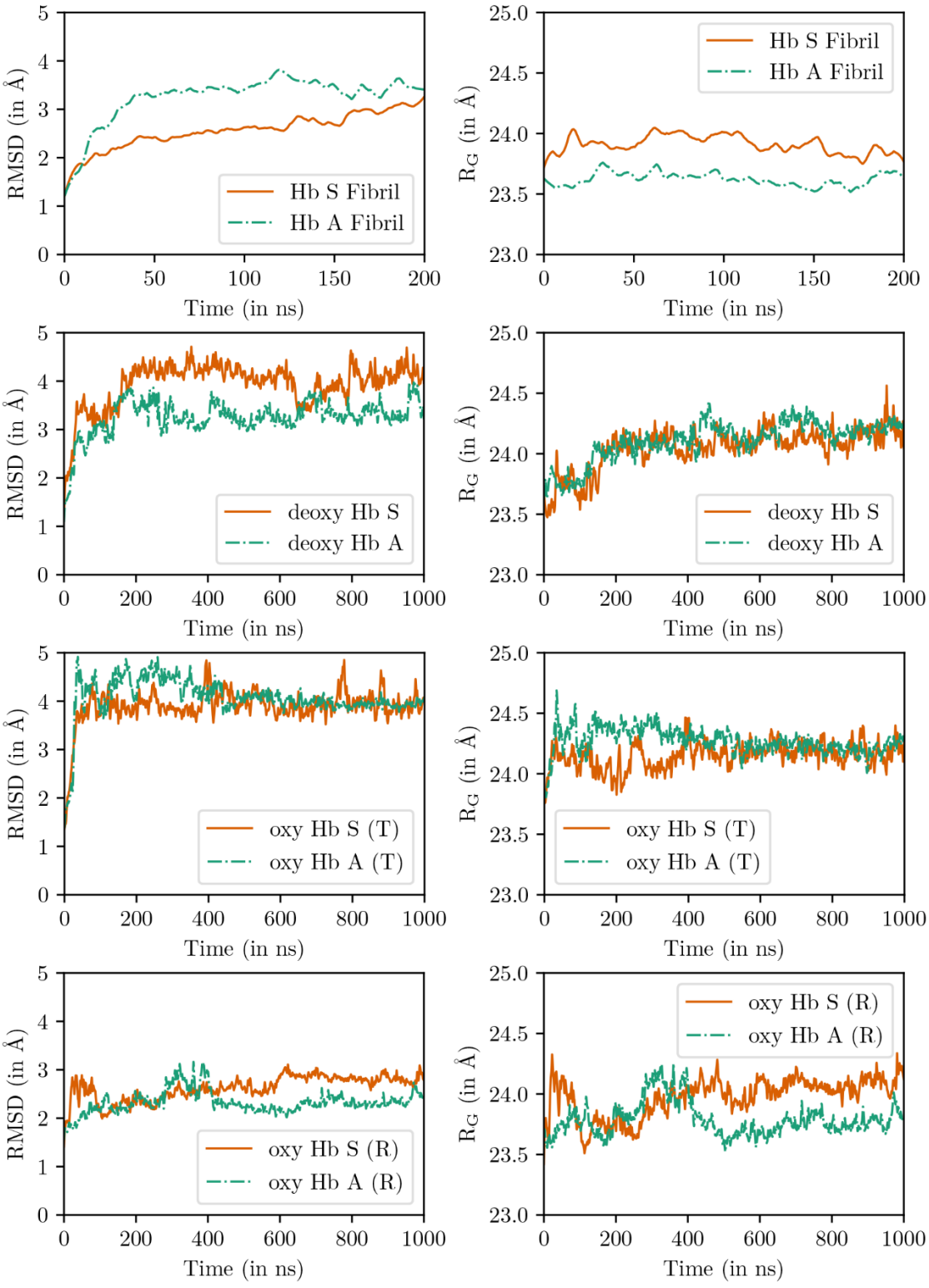

Figure S4. RMSD with respect to the respective crystal structure or starting model and radius of gyration (R_G) from the hemoglobin MD simulations. Savitzky-Golay filter with a window size of 1001 and a polynomial of degree 2 was applied to smooth the data.

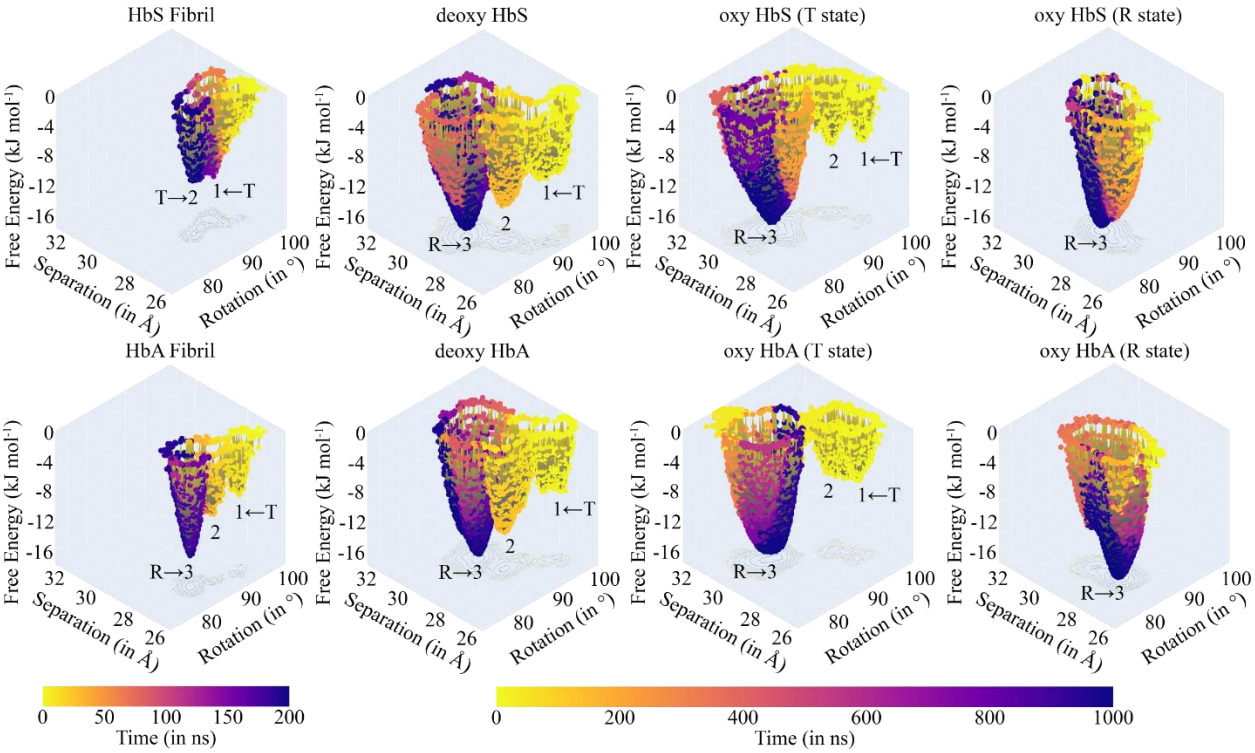

Figure S5. Free energy landscapes of hemoglobin evaluated using dimer-dimer rotation and separation. The landscapes are in the same range for each case, with 100 bins in each dimension. The trajectory points are plotted on the surface and colored according to the time given in the color bars. The landscapes for the fibril models are smaller because they were generated using 20,000 frames, while the others used 200,000 frames. The wells close to the dimer-dimer rotation of 85° are in R state, and the wells closer to 98° are in T state. The wells are labeled 1, 2, and 3 in the order in which these are visited. Hence, wells with the same label have a similar location. Each well has been labeled T or R state based on the dimer-dimer rotation; the well in the two oxyhemoglobin simulations starting from the R state remained in the R state and is labelled '3' because well-3 in all other cases was determined to be in R state. These landscapes confirm the information gained from the RMSD-R_G landscapes.

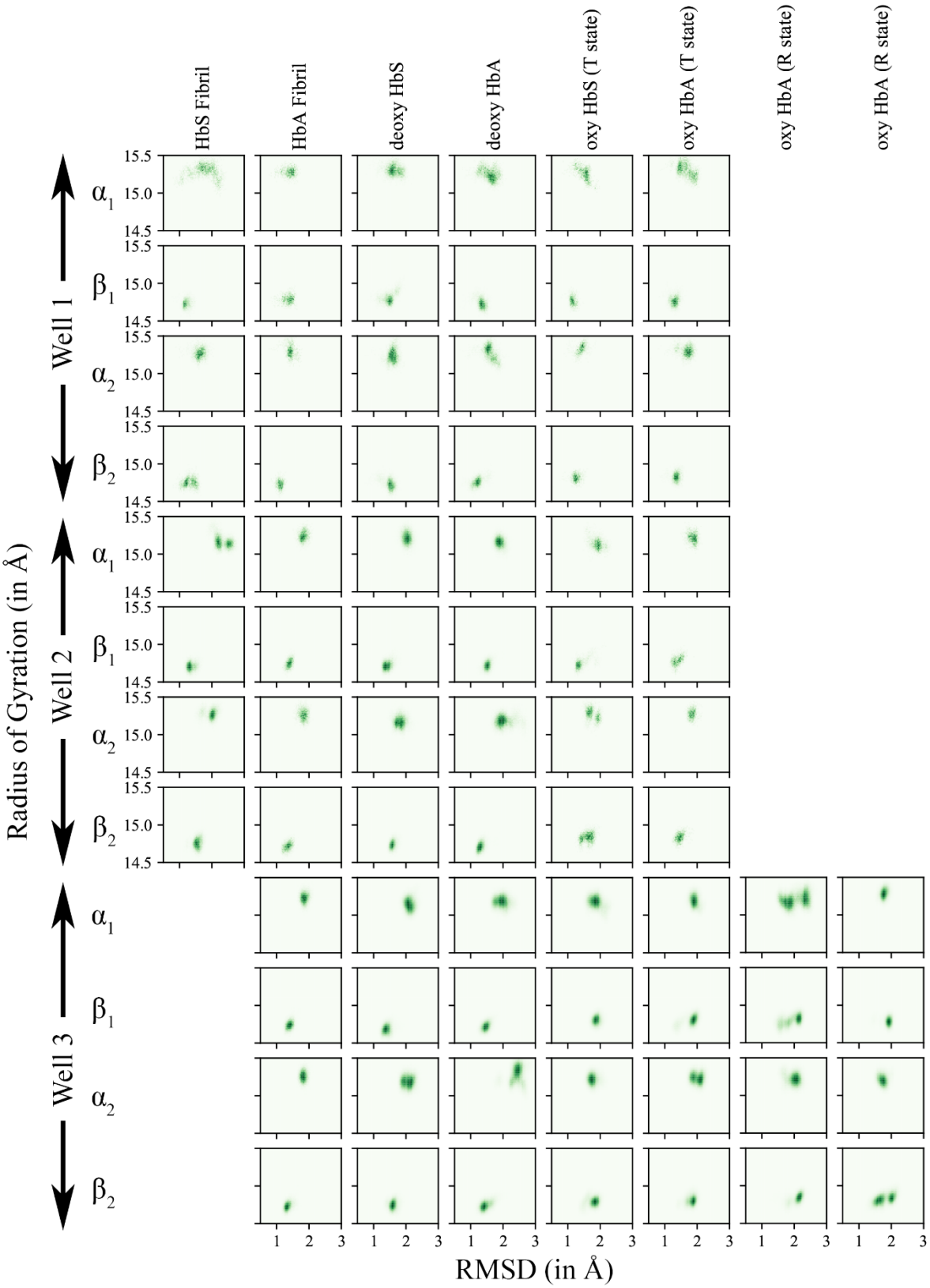

Figure S6. 2D histograms from RMSD and R_G of each hemoglobin subunit for the frames corresponding to each potential well in the free energy landscapes of hemoglobin.

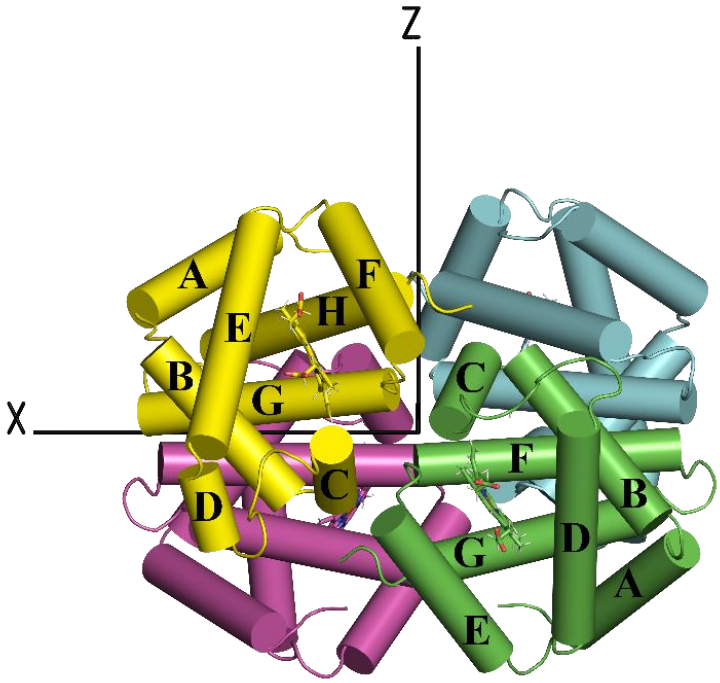

Figure S7. Structure of hemoglobin with the helices in α_1 and β_2 labeled. The molecule has its center of mass at the origin. The first, second, and third principal axes (corresponding to the principal moments of inertia) are aligned with x, y, and z, respectively, with the y-axis pointing out of the page. The chains are colored as follows: α_1=Green, β_1=Cyan, α_2=Magenta, and β_2=Yellow.

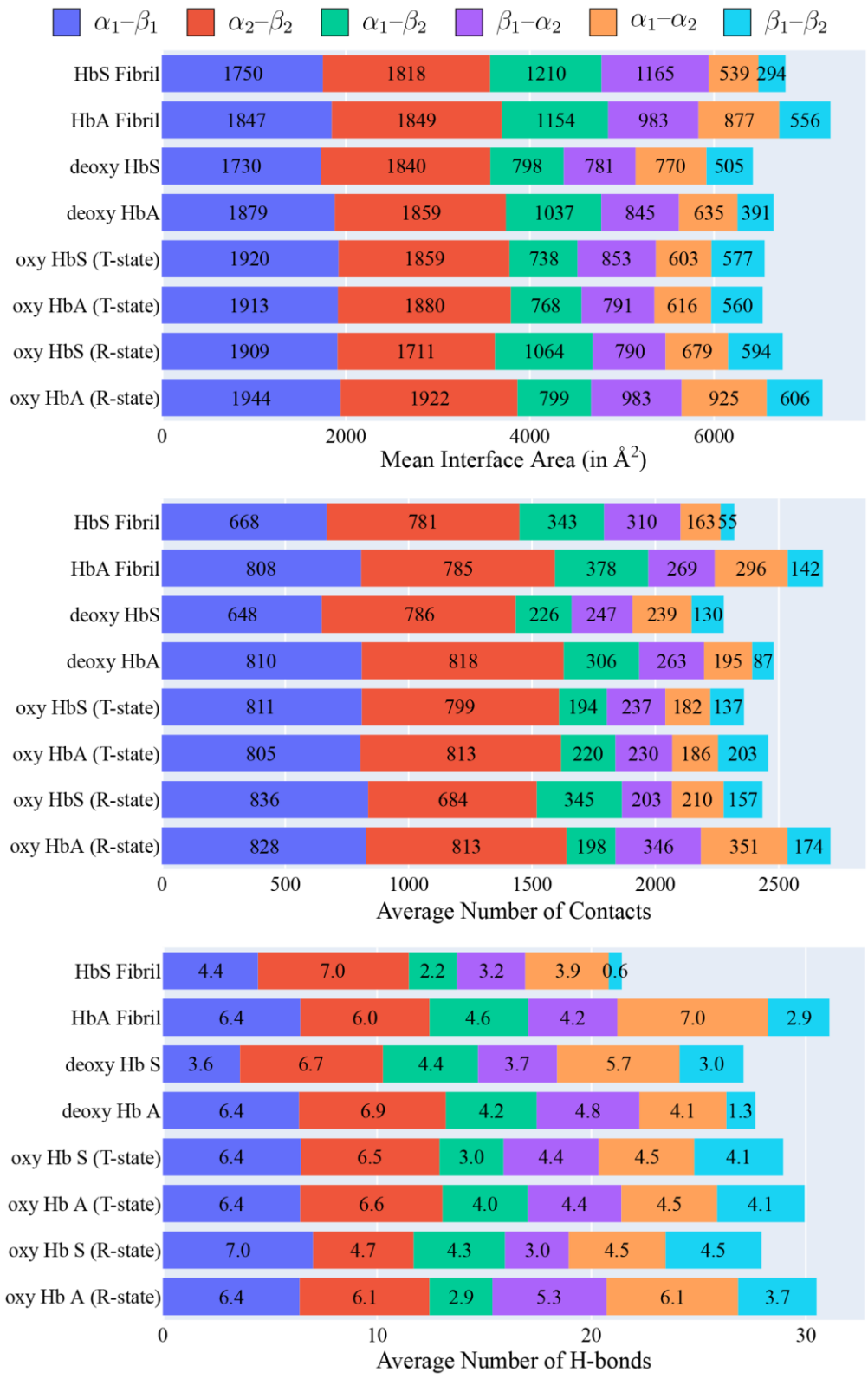

Figure S8. Intersubunit interface properties in hemoglobin averaged over the MD trajectory. In the fibril simulations, the area between the chain of the central molecule is listed above. Contacts are defined as pairs of atoms within 4 Å of each other.

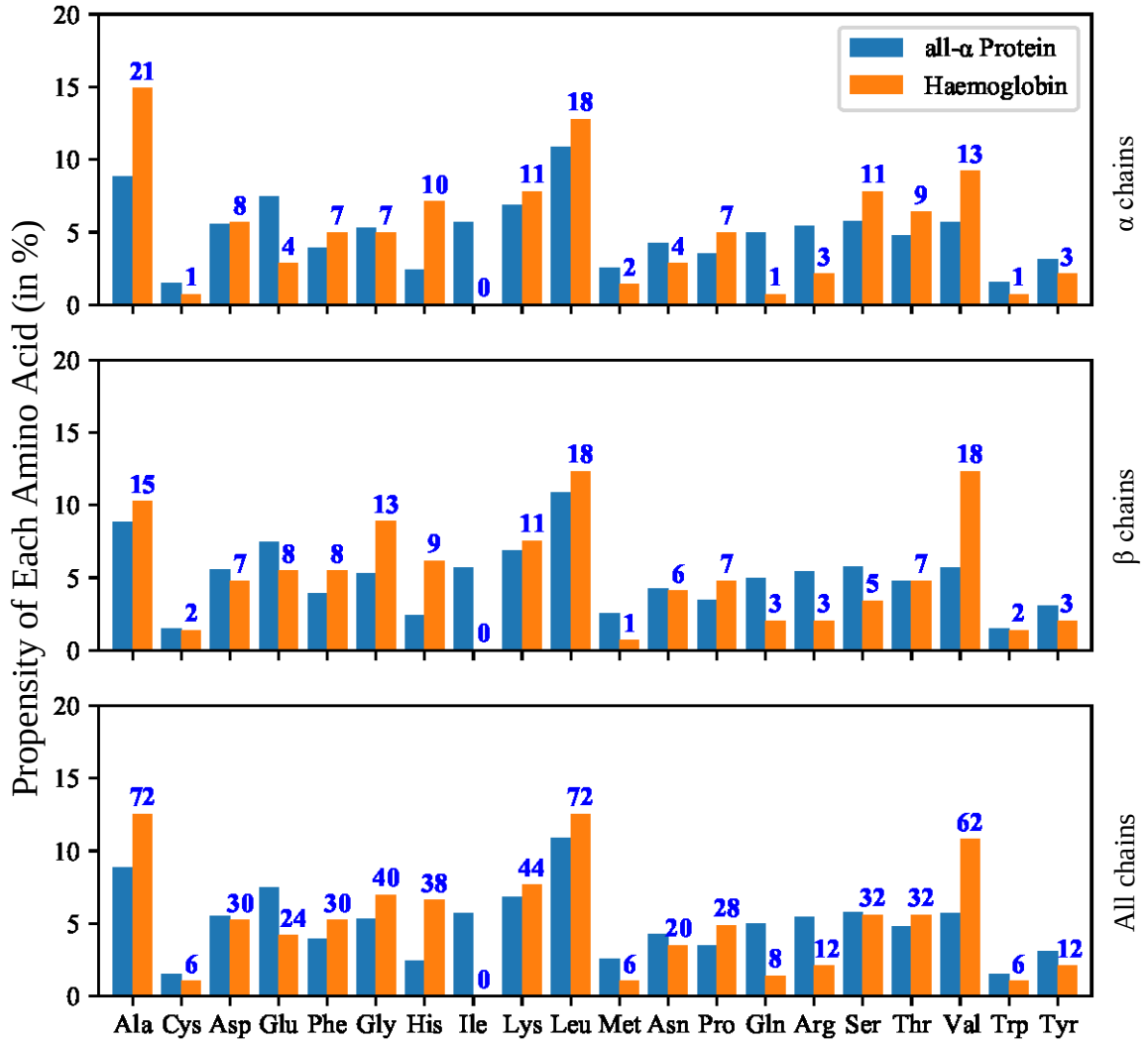

Figure S9. Amino acid composition of hemoglobin. The absolute number of each amino acid is given above the respective bars. The blue bars are the expected propensity of each amino acid in all-α proteins,[10] and the orange bars are the values observed in normal hemoglobin.

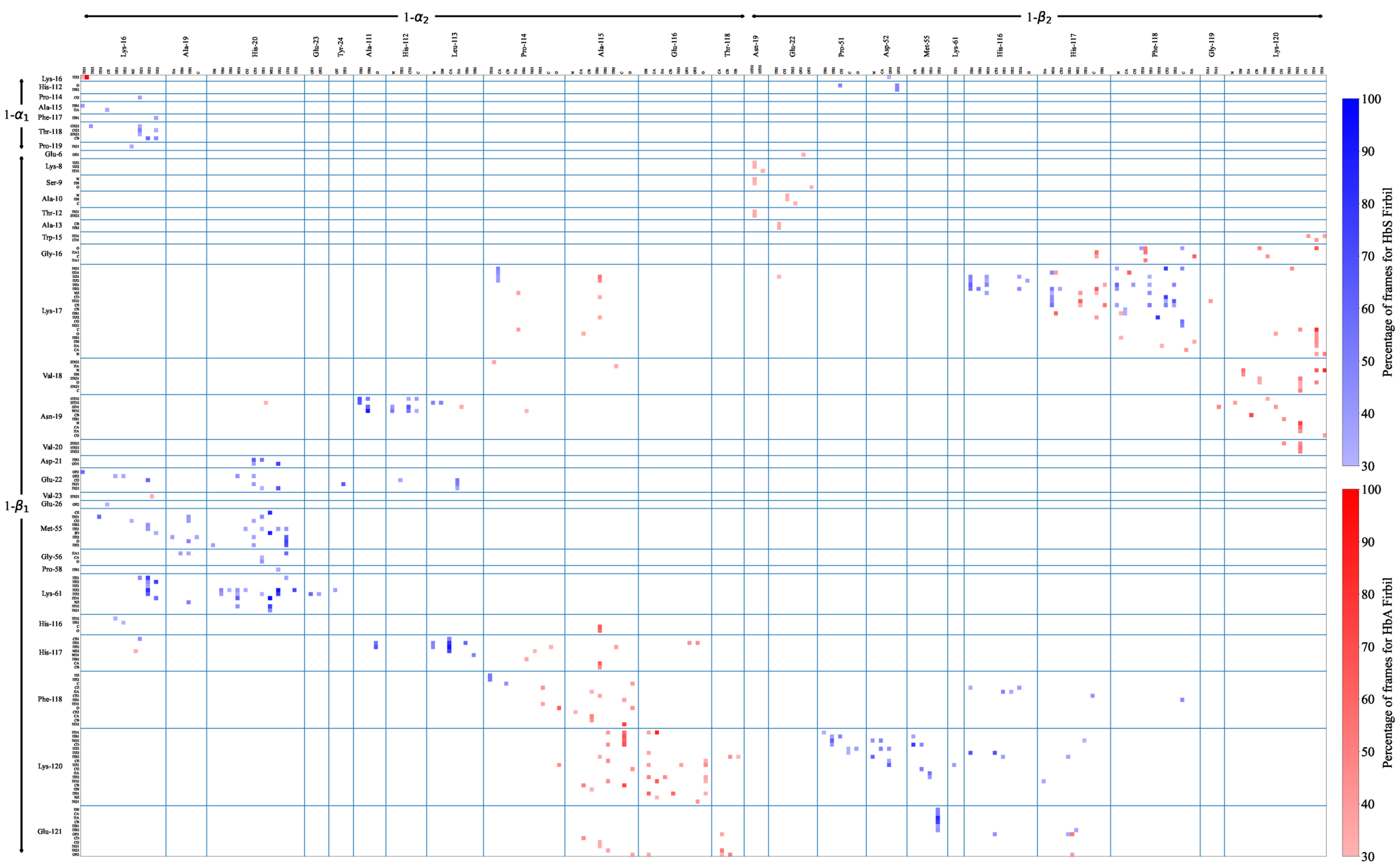

Figure S10. Axial contacts in the first strand of deoxy-HbS (crystal contacts after translation by 1 unit along x). The rows and columns give the atoms involved in the contact, and each atom label is for one and two points, respectively. The contacts in HbS fibril are in blue, and the contacts for HbA fibril are in red to the right of the corresponding contact. The brightness of the color gives the percentage of occurrence in the trajectory.

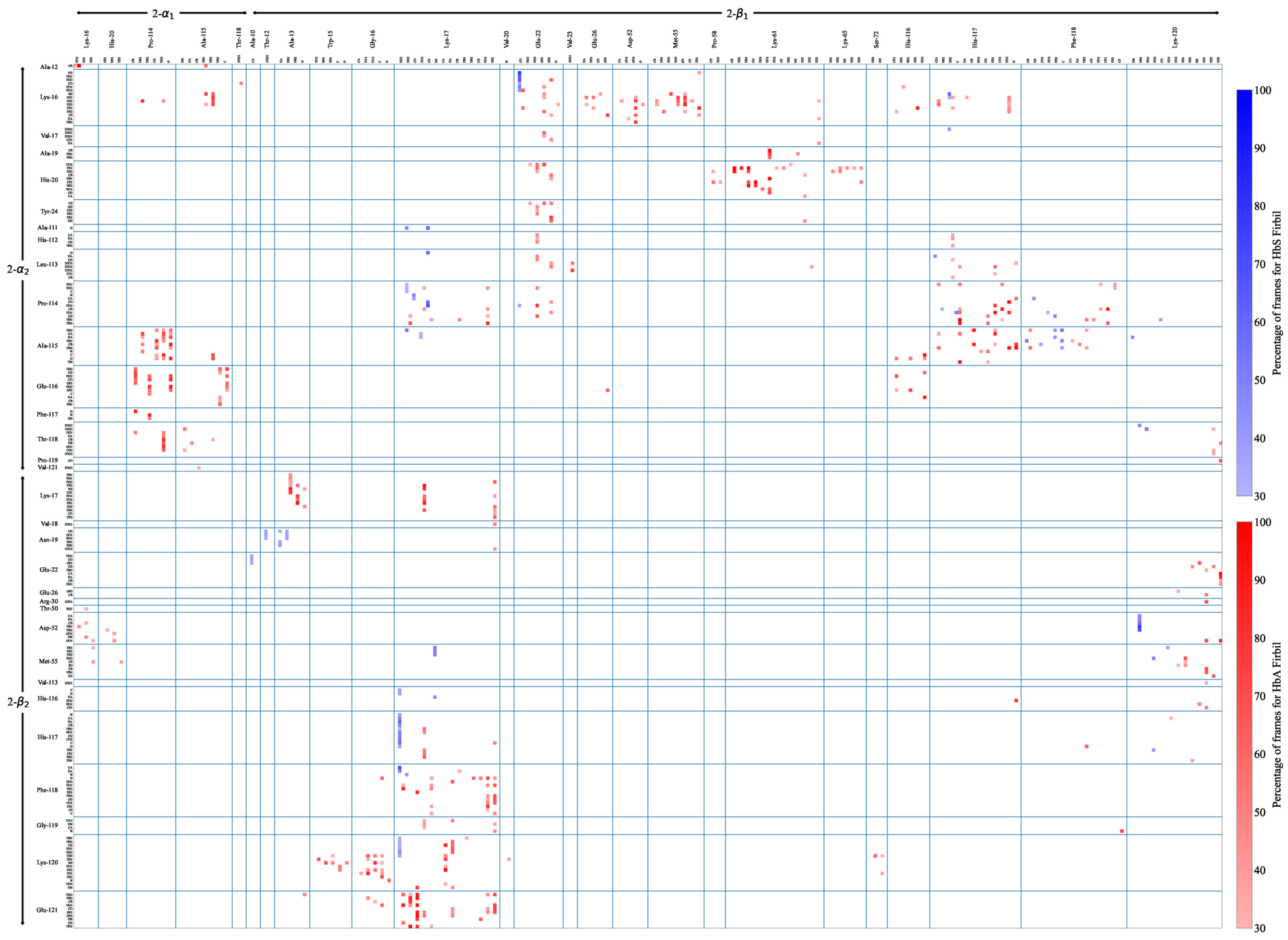

Figure S11. Axial contacts in the second strand of deoxy-HbS (crystal contacts after translation by −1 unit along x). The rows and columns give the atoms involved in the contact, and each atom label is for one and two points, respectively. The contacts in HbS fibril are in blue, and the contacts for HbA fibril are in red to the right of the corresponding contact. The brightness of the color gives the percentage of occurrence in the trajectory.

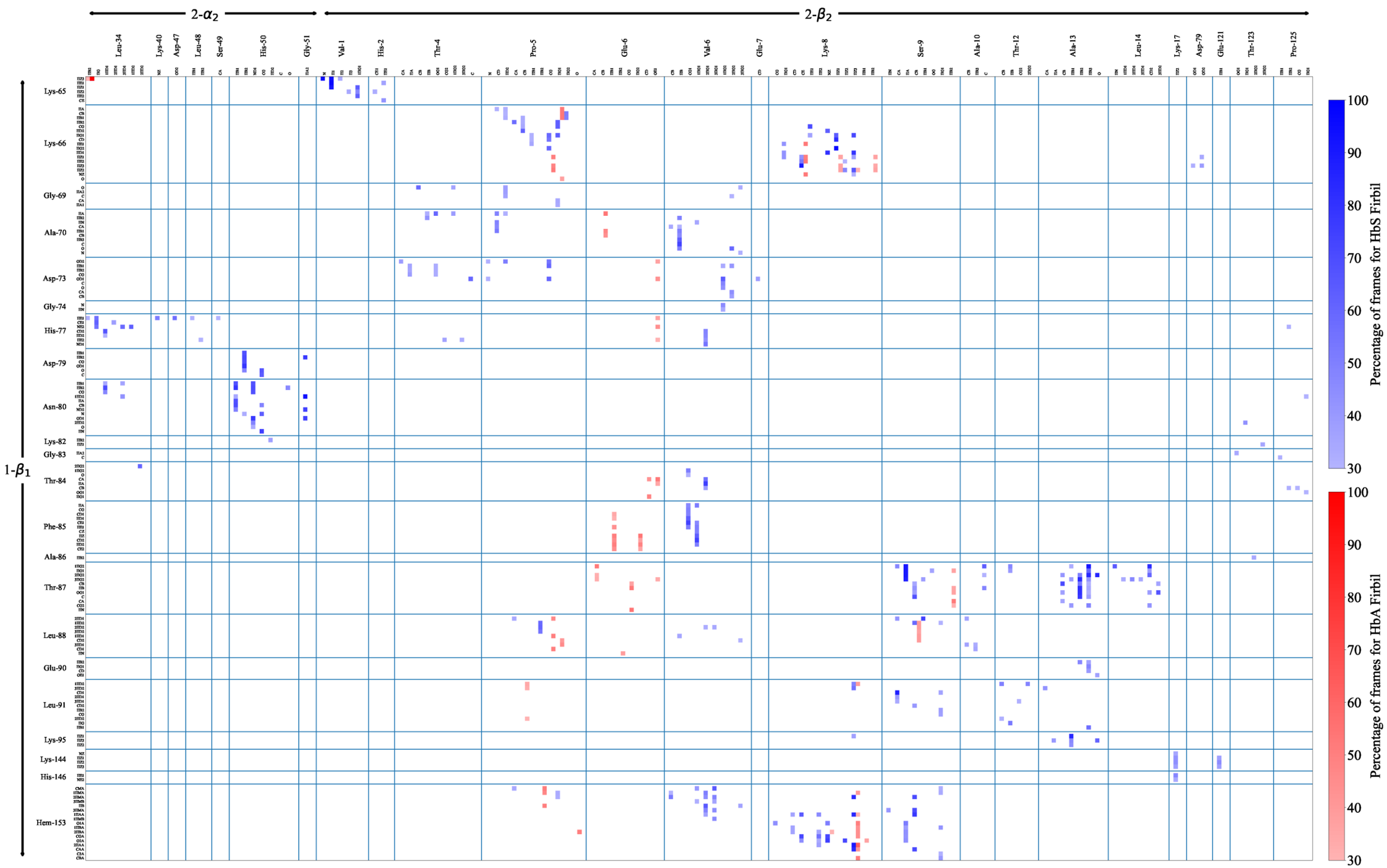

Figure S12. Lateral contacts between the two strands of deoxy-HbS (crystal contacts between the two independent tetramers in the asymmetric unit). The rows and columns give the atoms involved in the contact, and each atom label is for one and two points, respectively. The contacts in HbS fibril are in blue, and the contacts for HbA fibril are in red to the right of the corresponding contact. The brightness of the color gives the percentage of occurrence in the trajectory. Val- 6 is listed to the right of Glu-6 as a separate residue, but only one is present in a molecule; Val-6 in HbS Fibril and Glu-6 in HbA fibril.

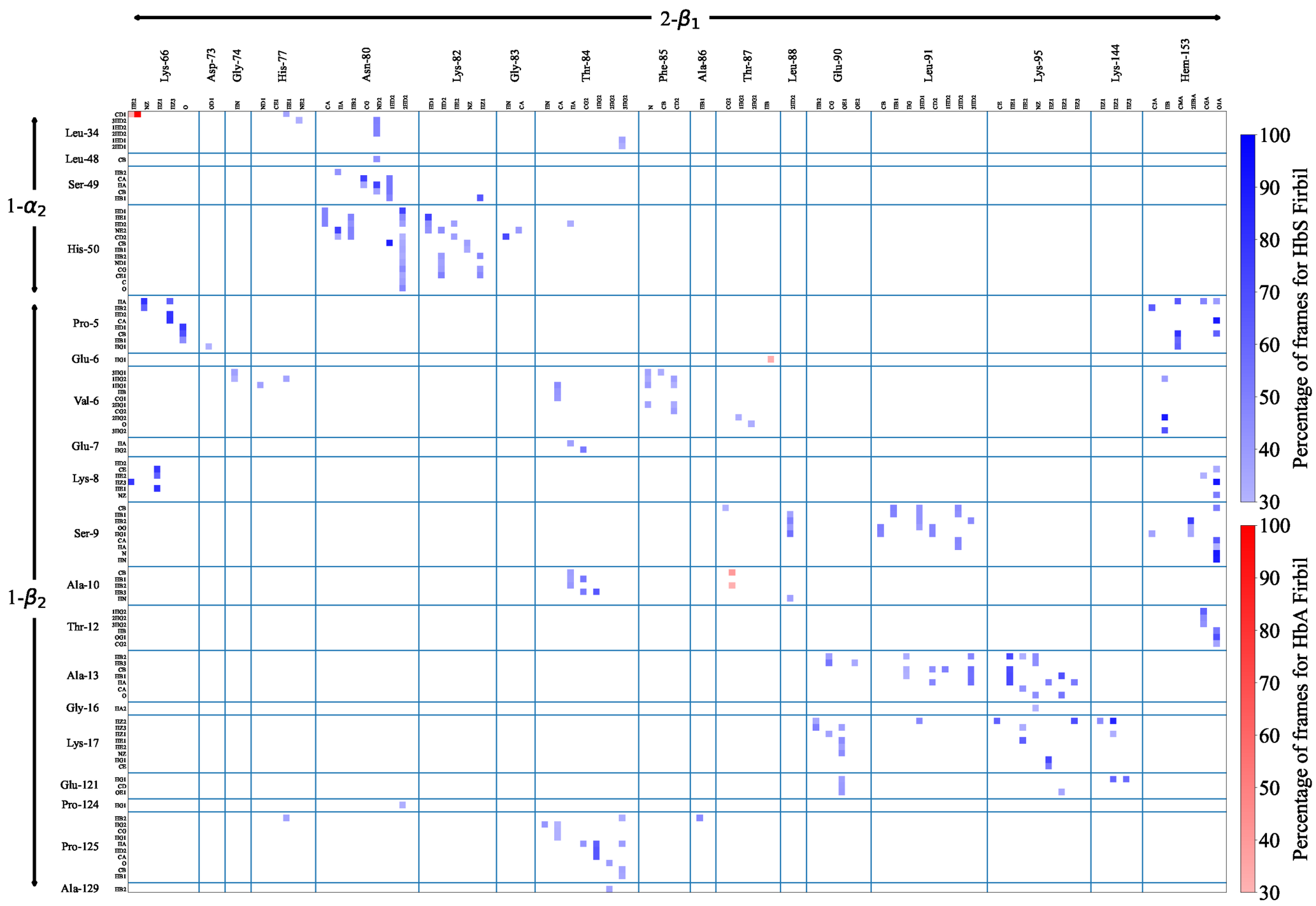

Figure S13. Lateral contacts between the two strands of deoxy-HbS (crystal contacts between the second tetramer in the asymmetric unit and the first tetramer after translation by −1 unit along x). The rows and columns give the atoms involved in the contact, and each atom label is for one and two points, respectively. The contacts in HbS fibril are in blue, and the contacts for HbA fibril are in red to the right of the corresponding contact. The brightness of the color gives the percentage of occurrence in the trajectory. Val- 6 is listed below Glu-6 as a separate residue, but only one is present in the molecule; Val-6 in HbS Fibril and Glu-6 in HbA fibril.

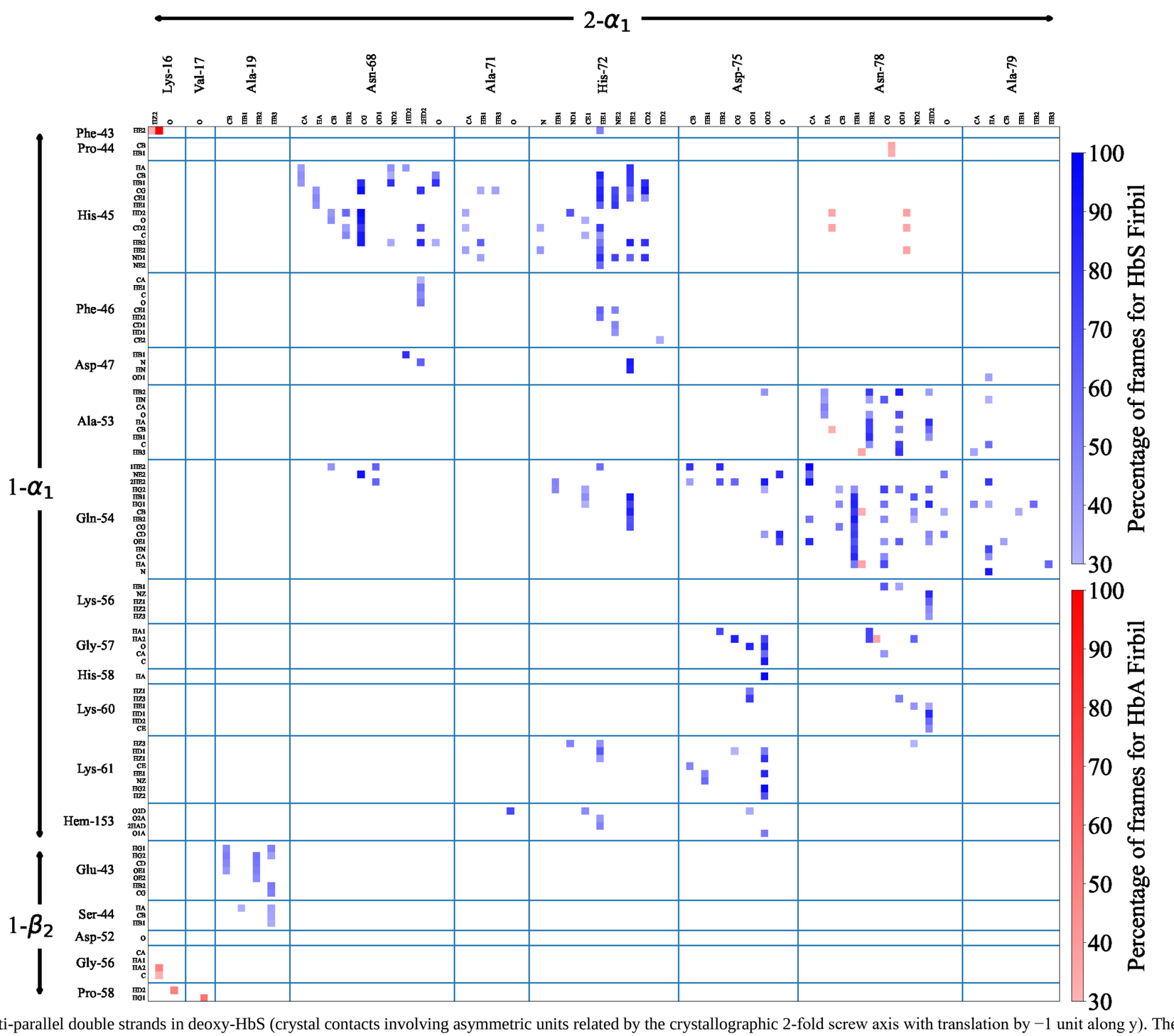

Figure S14. Contacts between anti-parallel double strands in deoxy-HbS (crystal contacts involving asymmetric units related by the crystallographic 2-fold screw axis with translation by −1 unit along y). The rows and columns give the atoms involved in the contact, and each atom label is for one and two points, respectively. The contacts in HbS fibril are in blue, and the contacts for HbA fibril are in red to the right of the corresponding contact. The brightness of the color gives the percentage of occurrence in the trajectory.

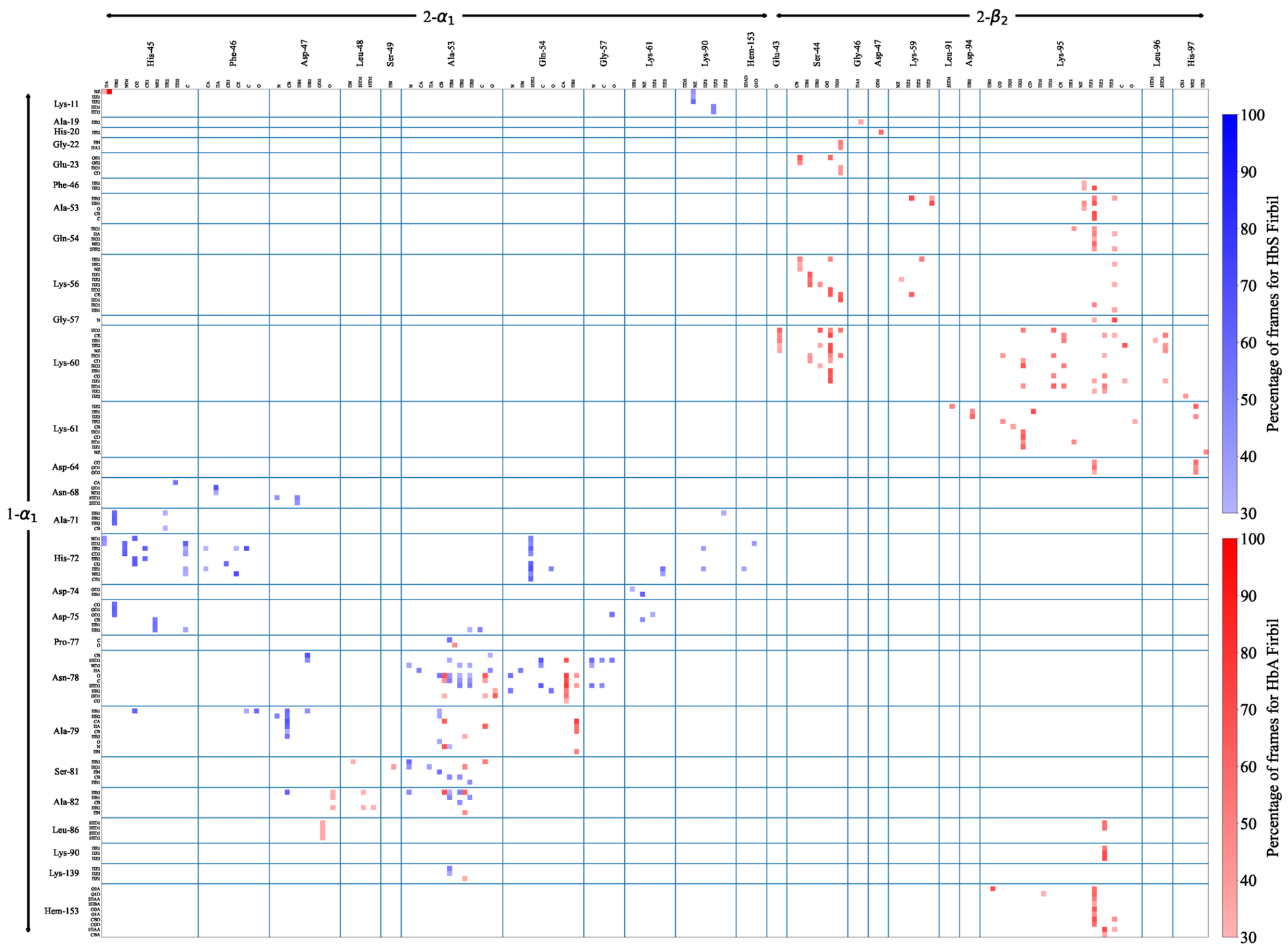

Figure S15. Contacts between anti-parallel double strands in deoxy-HbS (crystal contacts between asymmetric units related by the crystallographic 2-fold screw axis with a translation of −1 unit along y and −1 unit along z). The rows and columns give the atoms involved in the contact, and each atom label is for one and two points, respectively. The contacts in HbS fibril are in blue, and the contacts for HbA fibril are in red to the right of the corresponding contact. The brightness of the color gives the percentage of occurrence in the trajectory.

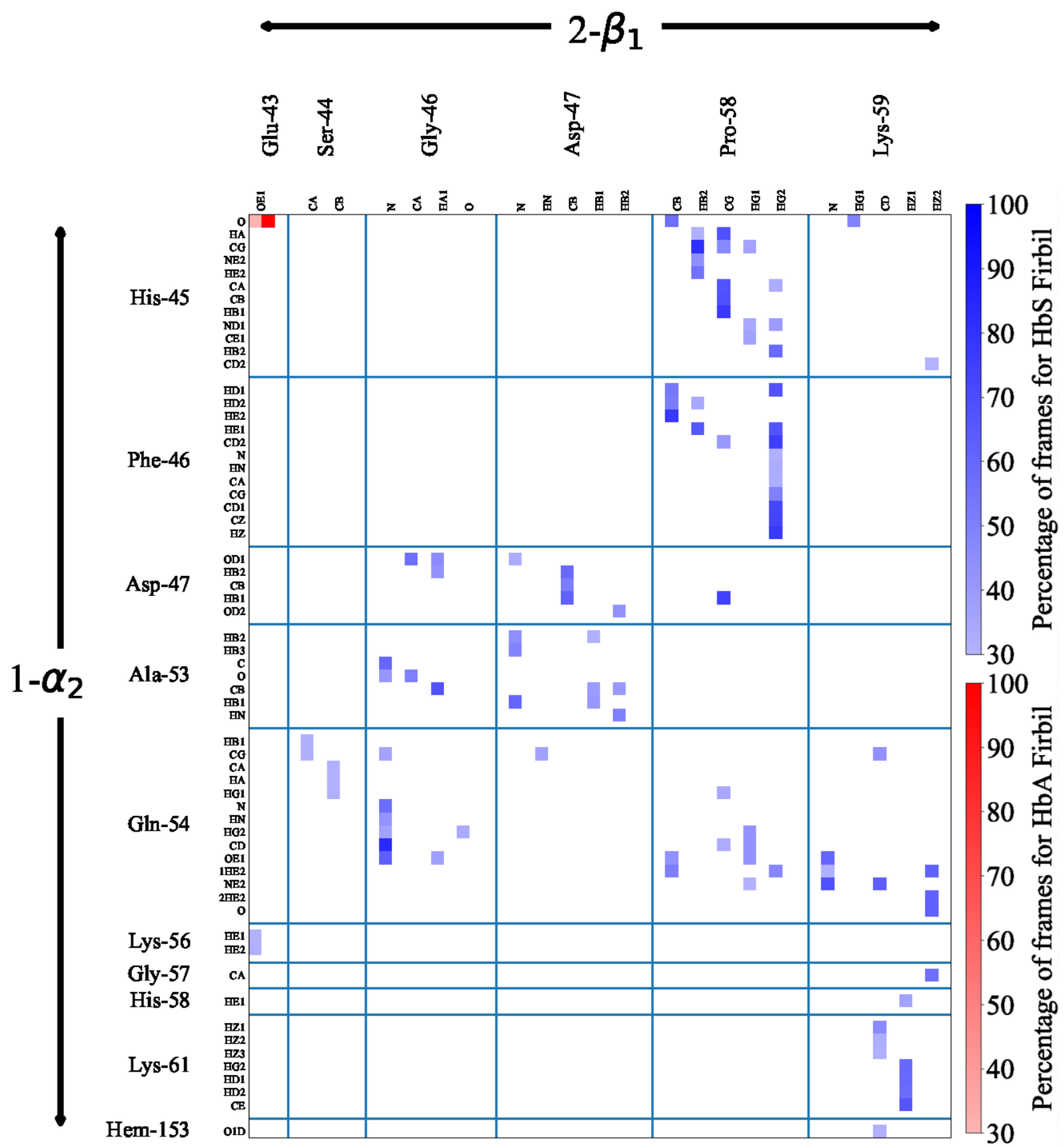

Figure S16. Contacts between parallel double strands in deoxy-HbS (crystal contacts after translation by −1 unit along x and −1 unit along z). The rows and columns give the atoms involved in the contact, and each atom label is for one and two points, respectively. The contacts in HbS fibril are in blue, and the contacts for HbA fibril are in red to the right of the corresponding contact. The brightness of the color gives the percentage of occurrence in the trajectory.

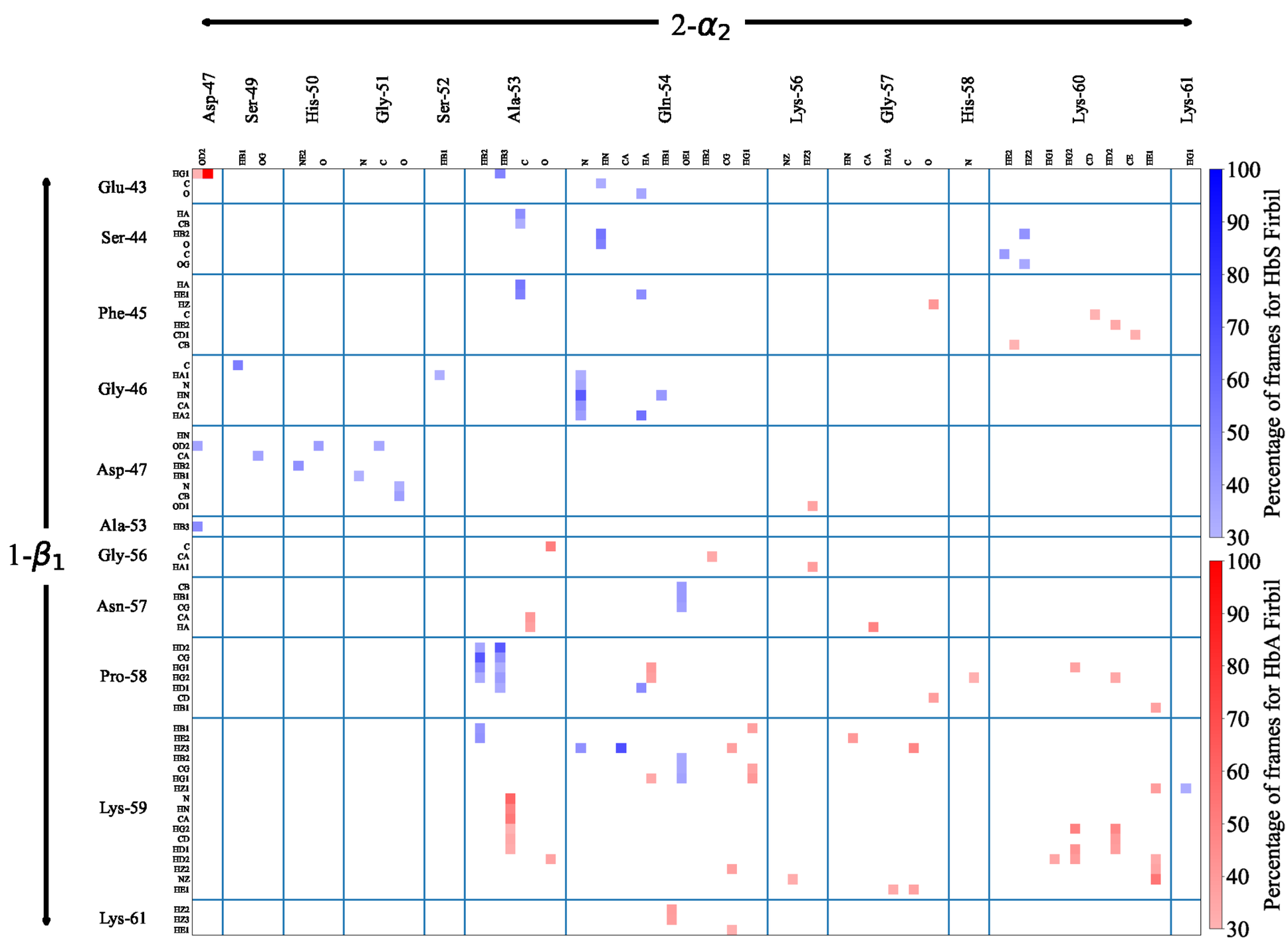

Figure S17. Contacts between parallel double strands in deoxy-HbS (crystal contacts between first and second tetramer after translation by −1 unit along z). The rows and columns give the atoms involved in the contact, and each atom label is for one and two points, respectively. The contacts in HbS fibril are in blue, and the contacts for HbA fibril are in red to the right of the corresponding contact. The brightness of the color gives the percentage of occurrence in the trajectory.

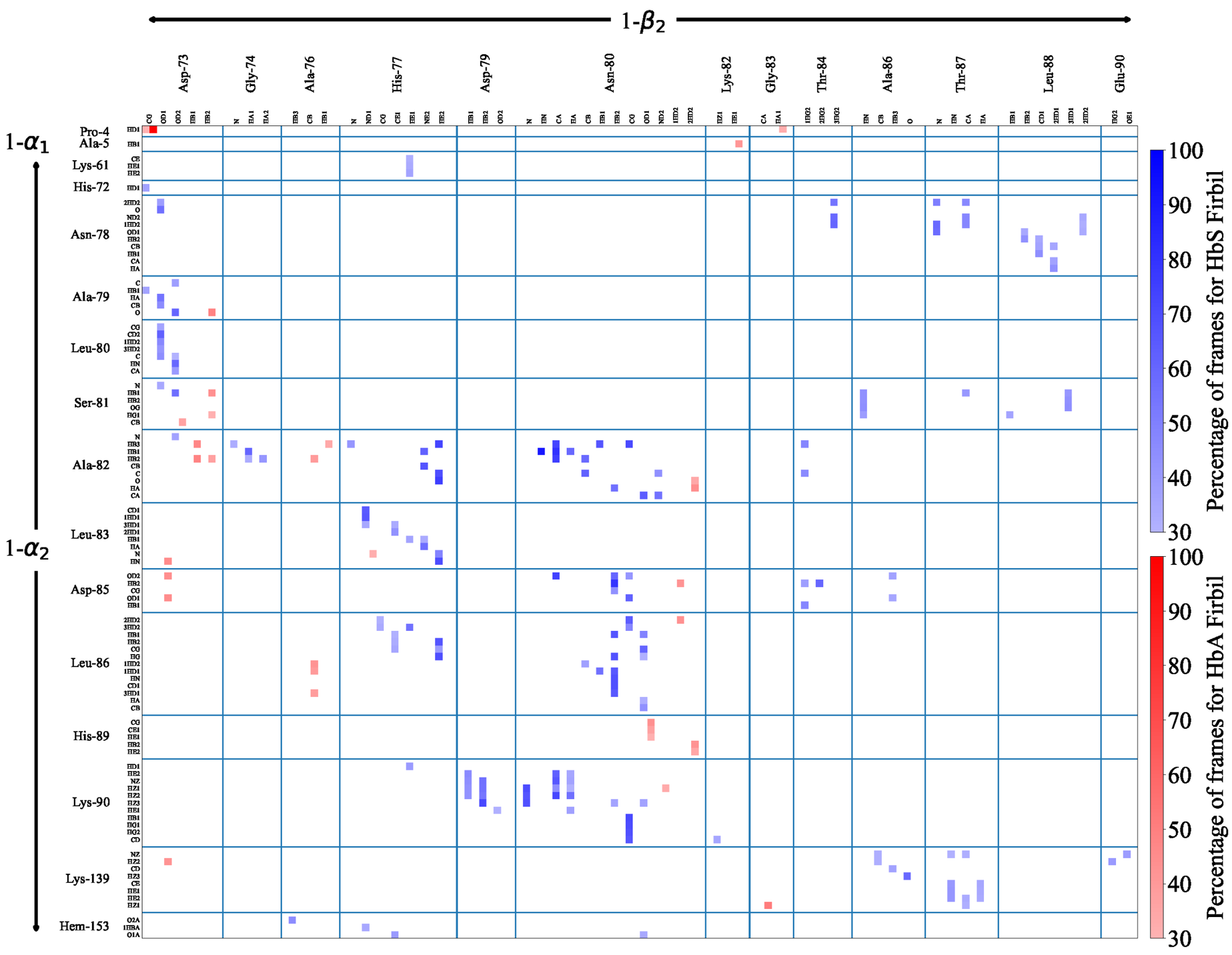

Figure S18. Contacts between parallel double strands in deoxy-HbS (crystal contacts between first tetramers after translation by −1 unit along z). The rows and columns give the atoms involved in the contact, and each atom label is for one and two points, respectively. The contacts in HbS fibril are in blue, and the contacts for HbA fibril are in red to the right of the corresponding contact. The brightness of the color gives the percentage of occurrence in the trajectory.

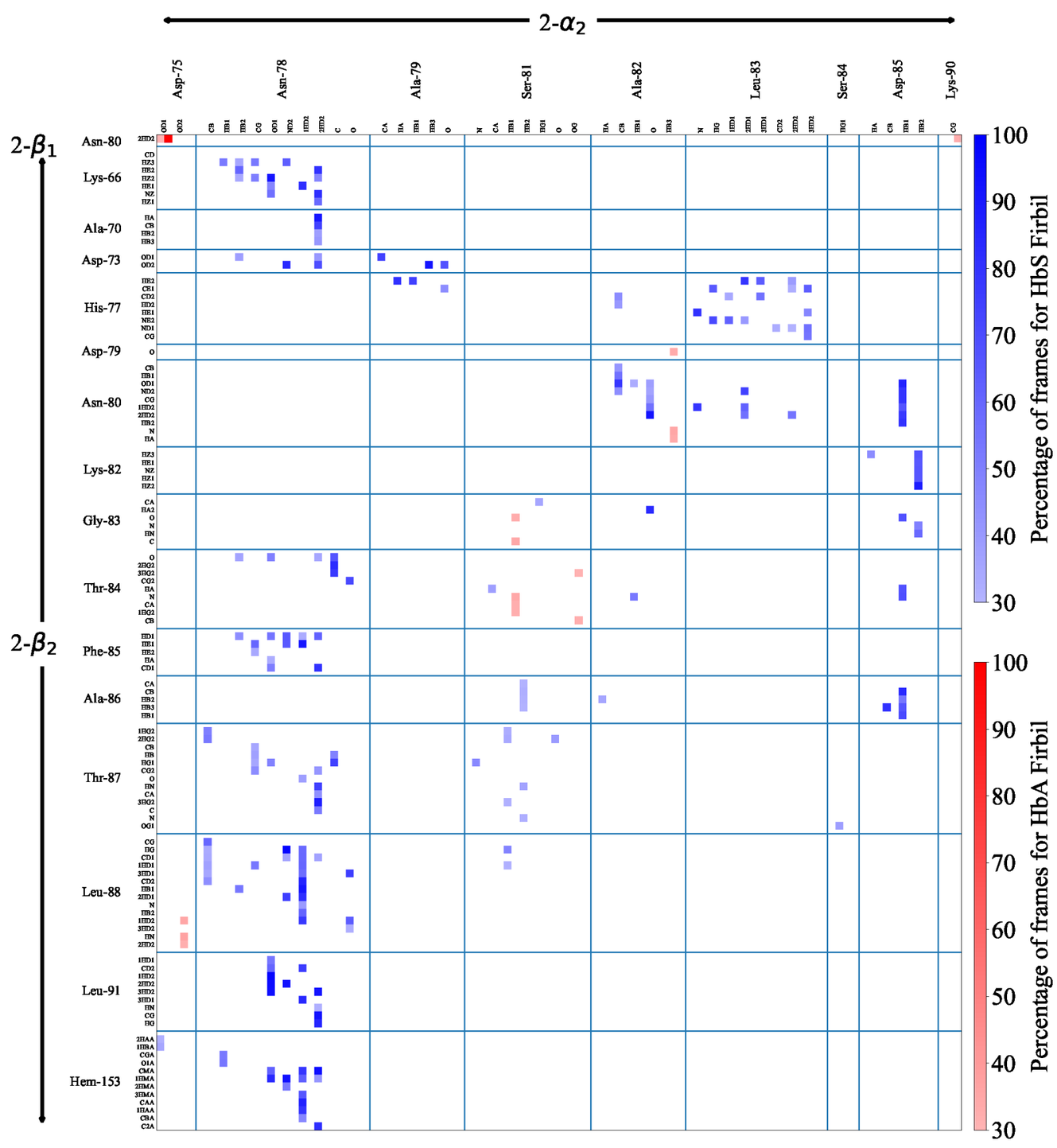

Figure S19. Contacts between parallel double strands in deoxy-HbS (crystal contacts between second tetramers after translation by −1 unit along z). The rows and columns give the atoms involved in the contact, and each atom label is for one and two points, respectively. The contacts in HbS fibril are in blue, and the contacts for HbA fibril are in red to the right of the corresponding contact. The brightness of the color gives the percentage of occurrence in the trajectory.

References:

1. Bringas, M.; Petruk, A. A.; Estrin, D. A.; Capece, L.; Martí, M. A., Tertiary and quaternary structural basis of oxygen affinity in human hemoglobin as revealed by multiscale simulations. *Scientific Reports* **2017,** *7* (1), 10926.

2. Galamba, N.; Pipolo, S., On the Binding Free Energy and Molecular Origin of Sickle Cell Hemoglobin Aggregation. *The Journal of Physical Chemistry B* **2018,** *122* (30), 7475-7483.

3. Galamba, N., On the Nonaggregation of Normal Adult Hemoglobin and the Aggregation of Sickle Cell Hemoglobin. *The Journal of Physical Chemistry B* **2019,** *123* (50), 10735-10745.

4. Carragher, B.; Bluemke, D. A.; Gabriel, B.; Potel, M. J.; Josephs, R., Structural analysis of polymers of sickle cell hemoglobin: I. Sickle hemoglobin fibers. *Journal of Molecular Biology* **1988,** *199* (2), 315-331.

5. Crepeau, R. H.; Dykes, G.; Garrell, R.; Edelstein, S. J., Diameter of haemoglobin S fibres in sickled cells. *Nature* **1978,** *274* (5671), 616.

6. Cretegny, I.; Edelstein, S. J., Double Strand Packing in Hemoglobin S Fibers. *Journal of Molecular Biology* **1993,** *230* (3), 733-738.

7. Dykes, G.; Crepeau, R. H.; Edelstein, S. J., Three-dimensional reconstruction of the fibres of sickle cell haemoglobin. *Nature* **1978,** *272* (5653), 506.

8. Dykes, G. W.; Crepeau, R. H.; Edelstein, S. J., Three-dimensional reconstruction of the 14-filament fibers of hemoglobin S. *Journal of Molecular Biology* **1979,** *130* (4), 451-472.

9. Garrell, R. L.; Crepeau, R. H.; Edelstein, S. J., Cross-Sectional Views of Hemoglobin S Fibers by Electron Microscopy and Computer Modeling. *Proceedings of the National Academy of Sciences of the United States of America* **1979,** *76* (3), 1140-1144.

10. Costantini, S.; Colonna, G.; Facchiano, A. M., Amino acid propensities for secondary structures are influenced by the protein structural class. *Biochemical and Biophysical Research Communications* **2006,** *342* (2), 441-451.